

**The Attributes of a Variable-Diameter Rotor
System Applied to Civil Tiltrotor Aircraft**

**NASA University Consortium Grant
NCC2-5174**

by

**Scott Brender
Graduate Student
The University of Texas at Austin**

**Hans Mark
Professor
Department of Aerospace Engineering and Engineering Mechanics
The University of Texas at Austin**

and

**Frank Aguilera
Advanced Tiltrotor Transport Technology Project Office
NASA Ames Research Center**

The Attributes of a Variable-Diameter Rotor System Applied to Civil Tiltrotor Aircraft

by

**Scott Brender
Graduate Student
The University of Texas at Austin**

**Hans Mark
Professor
Department of Aerospace Engineering and Engineering Mechanics
The University of Texas at Austin**

and

**Frank Aguilera
Advanced Tiltrotor Technology Project Office
NASA Ames Research Center**

The attributes of a variable-diameter rotor concept applied to civil tiltrotor aircraft are investigated using the V/STOL Aircraft Sizing and Performance Computer Program (VASCOMP). To begin, civil tiltrotor viability issues that motivate advanced rotor designs are discussed. Current work on the variable-diameter rotor and a theoretical basis for the advantages of the rotor system are presented. The size and performance of variable-diameter and conventional tiltrotor designs for the same baseline mission are then calculated using a modified, NASA Ames version of VASCOMP. The aircraft are compared based on gross weight, fuel required, engine size and autorotative performance for various hover disk loading values. Conclusions about the viability of the resulting designs are presented and a program for further variable-diameter rotor research is recommended.

Table of Contents

Abstract	ii
Table of Contents	iii
List of Tables.....	vi
List of Figures	vii
1. Introduction.....	1
1.1 Civil Tiltrotor Background	2
1.2 The Motivation for a Civil Tiltrotor.....	3
1.3 Civil Tiltrotor Viability Issues.....	5
1.3.1 Meeting Safety Standards.....	6
1.3.2 Meeting Environmental Standards	10
1.3.3 Economic Viability.....	11
1.3.4 Key Technologies for Tiltrotor Viability	14
2. The Variable-Diameter Rotor Concept	16
2.1 Variable-Geometry Background	18
2.2 Possible Variable-Diameter Designs.....	20

2.3	Recent Variable-Diameter Rotor Research	25
2.4	Variable-Diameter Rotor Complexity.....	27
3.	Advantages of a Variable-Diameter Rotor System	29
3.1	Introduction.....	29
3.2	Advantages in Hover	30
3.2.1	Induced Power	30
3.2.2	Figure of Merit	36
3.2.3	Rotor-Airframe Interactions.....	40
3.2.4	Summary of Hover Benefits.....	46
3.3	Advantages During Cruise.....	46
3.3.1	Rotor Propulsive Efficiency	46
3.3.2	Gust Response	55
3.4	Improved Autorotation Capability	55
3.5	External and Internal Noise.....	70
3.5.1	Harmonic Noise.....	70
3.5.2	Blade-Vortex Interaction	71
3.5.3	Internal Noise.....	72
4.	Aircraft Size and Performance Comparison Setup	73
4.1	VASCOMP	74
4.1.1	VASCOMP Sizing.....	74
4.1.2	VASCOMP Weight Estimation.....	76

4.1.3	VASCOMP Aerodynamics.....	79
4.1.4	VASCOMP Propulsion.....	80
4.1.5	VASCOMP Conversion and Download.....	82
4.2	Comparison Approach	83
4.2.1	Common VASCOMP Inputs	84
4.2.2	Variable-Diameter Tiltrotor VASCOMP Model.....	86
4.2.3	Conventional Tiltrotor VASCOMP Model	89
5.	Results	91
5.1	Baseline Aircraft Comparisons.....	91
5.2	Comparison Over a Range of Hover Disk Loading.....	97
6.	Conclusions and Recommendations.....	107
6.1	Conclusions.....	107
6.2	Recommended Research	110
	Bibliography	113

List of Tables

5.1	Baseline Conventional and Variable-Diameter Design Summary	92
5.2	Conceptual Design Dimension Information	100

List of Figures

1.1 Total Trip Time vs. Design Cruise Speed	12
1.2 CTR Productivity Index vs. Design Cruise Speed	12
1.3 CTR Baseline Mission Profile	13
1.4 Cabin Noise Levels of Various Aircraft.....	14
2.1 The Variable-Diameter Tiltrotor Concept	16
2.2 Disk Loading vs. Design Cruise Speed of Various Aircraft.....	18
2.3 Variable-Diameter Rotor Blade.....	20
2.4 Variable-Diameter Rotor Hub	22
2.5 Simple Model of the Variable-Diameter Rotor	23
2.6 Wind Tunnel Results for VDTR Figure of Merit	26
2.7 VDTR vs. Conventional Response to a 30 fps Wind Gust.....	36
3.1 Momentum Theory Control Volume	31
3.2 Conventional Tiltrotor Tip Clearance.....	34
3.3 Variable-Diameter Tiltrotor Tip Clearance	35
3.4 Forces Acting on an Airfoil During Hover	37
3.5 Figure of Merit vs. Propulsive Efficiency Trend	40
3.6 Download vs. C_T for a V-22 Tiltrotor.....	43
3.7 Beneficial Interference Effects for Low Rotor Shaft Spacing.....	45
3.8 Forces Acting on Airfoils in the Cruise Flight Mode.....	48
3.9 Rotor Compressibility Drag Factor.....	50

3.10 η_p vs. C_T/σ for a Constant Tip Speed.....	52
3.11 η_p vs. C_T/σ at Constant Thrust.....	52
3.12 Forces Acting on an Airfoil During Autorotation.....	56
3.13 Deadman's Curve for a Typical Rotorcraft.....	58
3.14 Blade Twist Comparisons.....	59
3.15 Forces During Autorotation in the Deceleration Region.....	60
3.16 The Aerodynamic Regions of a Rotor During Autorotation.....	61
3.17 The Autorotative Thrust Boundary of an, Isolated Conventional Rotor....	62
3.18 Autorotative Thrust Boundary of an Isolated Variable-Diameter Rotor.....	62
3.19 Power Required Curve for Helicopter Forward Flight.....	64
3.20 Momentum Theory Control Volume for Forward Flight.....	65
4.1 VASCOMP Conversion Acceleration Profile.....	85
4.2 Diameter vs. Nacelle Tilt Schedule.....	87
4.3 Nacelle Tilt vs. Forward Speed.....	88
5.1 Conventional Rotor Baseline Aircraft Weights.....	93
5.2 Variable-Diameter Rotor Baseline Aircraft Weights.....	93
5.3 VASCOMP Calculated Gross Weight vs. Disk Loading.....	101
5.4 VASCOMP Calculated Wing Weight.....	102
5.5 VASCOMP Calculated Wing Drag.....	103
5.6 VASCOMP Calculated Fuel Weight.....	104
5.7 VASCOMP Calculated Engine Weight.....	105
5.8 VASCOMP Calculated Acoustic Treatment Weight.....	105

Chapter 1

Introduction

Tiltrotor aircraft have the potential to revolutionize civil air transportation. A civil tiltrotor (CTR) could relieve growing congestion at airports while making air travel more convenient and accessible to passengers around the world. While tiltrotor research has been on going for decades, recent technologies such as advanced control systems and light weight composite structures now make a civil tiltrotor technically feasible. Additionally, the V-22, a tiltrotor designed for the Department of Defense, will be available in the near future to provide operational experience to facilitate the CTR design process. A program involving the joint efforts of government and industry to develop the infrastructure and remaining technologies required for a viable CTR could soon make these aircraft a reality.

Because tiltrotors are different from any aircraft currently used for civil transportation, several unique issues are involved in their viability. External noise levels, safety in forward and vertical flight modes, passenger comfort and operating costs could affect the success of the aircraft. It is imperative that a government and industry research program provide solutions to identified problems in these areas.

Many of the technical problems that arise from the requirements of a large civil tiltrotor could be solved by using variable-diameter rotors. These rotors change diameter in flight so that a large helicopter-size rotor is used in hover and a smaller propeller-like rotor is used in cruise. The low disk loading in hover and low tip

speeds in cruise made possible by the diameter change could eliminate many of the undesirable conventional tiltrotor attributes. Of course, these advantages do not come without a price. The diameter change mechanism adds weight and complexity to the rotor system which must be weighted against potential benefits.

The purpose of this study is to assess the impact variable-diameter tiltrotor aircraft could make on civil tiltrotor viability. The approach taken is to compare the performance advantages and weight penalties of conceptual tiltrotor aircraft equipped with variable-diameter rotors as calculated by the V/STOL Aircraft Sizing and Performance Computer Program (VASCOMP). The issue of variable-diameter rotor complexity is also discussed briefly, however, a true reliability analysis must await the design of actual rotor hardware and is beyond the scope of this study. To begin the analysis, the key issues affecting civil tiltrotor viability are discussed to establish the need for an advanced rotor design. In Chapter 2 the variable-diameter concept is introduced. The complexity of the extension and retraction mechanism is discussed briefly and much of the current research on the concept is presented. A theoretical justification for the advantages of the rotor system in hover, cruise, autorotation and noise are presented in Chapter 3. In Chapter 4 the details of the VASCOMP code and the VASCOMP inputs particular to this case are discussed. The results of the aircraft sizing are presented in Chapter 5. Finally, in Chapter 6, conclusions of this study and recommendations for future areas of research are presented.

1.1 Civil Tiltrotor Background

In recognition of the potential benefits of a CTR, government agencies have sponsored several studies to investigate CTR development. The first in depth study

was conducted for the National Aeronautics and Space Administration (NASA) and the Federal Aviation Administration (FAA) by the Boeing Airplane Company [1,2]. This two phase study was key in identifying configurations and mission profiles for a market responsive aircraft. Shortly thereafter, a High-Speed Rotorcraft Technology Task Force was appointed by NASA to further study the concept [3]. This committee, consisting of several senior members of the aerospace industry, identified technologies needed to ensure the safety, economic viability and community acceptance of tiltrotors. The most comprehensive study to date was conducted by the Civil Tiltrotor Development Advisory Committee (CTRDAC) which was formed by the Secretary of Transportation as directed by the U.S. Congress [4]. The CTRDAC was charged with several tasks which included examining the costs, technical feasibility, and economic viability of CTR aircraft, determining research and development and regulatory changes needed to integrate the CTR into the national transportation system and deciding how funding for CTR development should be divided by government and industry. Each of these studies concluded that society stands to benefit substantially from a transportation system made possible by tiltrotor aircraft.

1.2 The Motivation for a Civil Tiltrotor

Perhaps the single most important benefit of a civil tiltrotor will be to make air travel more convenient. With contemporary forms of commercial aviation, passengers making trips of less than 700 miles typically spend fifty percent of their total travel time on the ground [4]. Time spent traveling to and from an airport, checking in, and waiting on the taxiway could be reduced by a vertical flight capability. For ranges of

less than 600 miles, tiltrotors could actually lead to shorter travel times than modern jetliners, since at this distance, travel time is dominated by access and egress time rather than cruise speed [1]. Helicopters already have this capability, but, for ranges over a few hundred miles, their advantage during take-off and landing is offset by limited forward speed and poor efficiency. In addition, helicopter high-speed flight involves vibration levels that reduce component reliability and aircraft safety. Unlike the helicopter, the tiltrotor converts to an airplane configuration during forward flight and will have a cruise performance comparable to a modern turboprop.

Tiltrotors are also a low cost solution to growing congestion problems at airports around the world. Airlines in the United States report that delays already cost themselves and their passengers more than \$3 billion dollars annually [4]. If the demand for air travel continues to outpace the national gross domestic product as predicted by the Federal Aviation Administration, congestion could reach crisis levels. Many of the delays experienced today stem from the high demand for short-haul flights. For example, in the northeastern United States, where average delays are among the longest, nearly sixty percent of flights originate from fewer than 500 nautical miles away [2]. For a low cost, tiltrotors could divert much of this traffic to free up runways for longer range jets. The estimated cost for CTR development and production including 20 vertiports is less than the cost of even one major hub airport [2]. Predicted annual time savings are on the order of 125,000 hours which translates into a \$375 million savings in passenger delay and aircraft operating costs [4].

A CTR could also expand the availability of air transportation. In many sparsely populated areas of the United States and around the world, no short-haul coverage exists. In these regions, for much less than what a small regional airport costs, a vertiport could provide tiltrotor feeder, transfer and line-haul services. These benefits

are particularly strong in countries such as China where the current infrastructure for conventional aircraft is inadequate to meet passenger demand for air travel.

Since the United States leads the world in tiltrotor technology, a CTR would probably be without competition for many years and could make a substantial impact on U.S. aircraft exports. In fact, more than fifty percent of CTR sales are expected to be in foreign markets [4]. Japan and a consortium of European countries are each designing their own civil VTOL aircraft to meet the transportation needs of their large populations. The Japanese have the Ishida tiltwing and the Europeans are designing the EUROFAR tiltrotor. The French, English and German aerospace industry consortium has set a goal of developing the EUROFAR for final certification by the year 2009 [4]. If industry in the U.S. does not capitalize on the potential market, others surely will.

1.3 Civil Tiltrotor Viability Issues

The advantages to society alone are not sufficient to motivate CTR production. A production decision will require some expectation of a transfer of wealth between manufactures and operators. Since these aircraft are so unique, costs and revenues are difficult to predict. Profits will be influenced by several factors including infrastructure development, certification standards, community acceptance, and passenger acceptance. This study focuses on aircraft related issues assuming that infrastructure will follow successful aircraft development.

The question of aircraft viability depends on whether an aircraft can be produced that meets passenger ride quality standards, federal safety standards and local environmental standards. Certainly passengers must feel comfortable and safe in

tiltrotors. To many passengers, comfort may be more important than convenience, and unless they feel safe in tiltrotors, they will continue to travel on jet aircraft. A CTR must also demonstrate the ability to meet safety regulations for eventual certification by the Federal Aviation Administration. This requires some forethought, as stated before, since firm certification standards do not yet exist for tiltrotor aircraft. Finally, a CTR must demonstrate an ability to meet environmental regulations. Of particular concern is the need to meet local noise standards since the tiltrotor is intended for use within populated areas rather than being confined to airports where aircraft noise is tolerated.

1.3.1 Meeting Safety Standards

Although currently only interim FAA regulations exist for tiltrotor aircraft, it has been assumed by the CTRDAC and others that a CTR will have to match the same levels of safety found in today's airliners [3, 4]. Since tiltrotors operate in both a fixed-wing and a helicopter mode, it follows that they will have to incorporate most, if not all, of the safety features of modern turboprops and helicopters. This implies that the aircraft must be capable of making controlled power-off and one engine inoperative (OEI) landings from vertical as well as level flight modes.

If one engine fails, a controlled landing will likely be possible if single engine power is distributed to both rotors through an interconnected drive shaft that runs through the aircraft wings as in the V-22. In a cruise configuration, the sharing of a single engine's power to both propellers would actually provide a safer situation than that found in modern twin-engine fixed-wing aircraft. In a conventional fixed-wing aircraft, the loss of one engine causes a coupled roll and yaw moment that can only be

balanced by the aircraft control surfaces above some minimum control airspeed. If both rotors in a CTR were interconnected, the loss of one engine would not cause an unbalance in the forces on the aircraft, and there would not be a minimum control speed other than the stall speed.

If one engine fails during a vertical flight mode such as conversion, takeoff or landing, the pilot could maneuver the aircraft over or around obstacles before selecting a suitable landing site as long as the remaining engine has sufficient power. The drawback to this scenario is that it requires the engines to be designed to produce nearly twice their normal operating power. Oversizing the engines adds weight and reduces fuel economy. The size of the engines can be reduced by taking advantage of the ability of turbine engines produce short bursts of power well above their normal rated power. However, the extent of engine damage when using this contingency power is unknown and engines must normally be replaced- an extremely expensive practice for large aircraft. Some studies suggest that to meet OEI requirements of CTR aircraft, new engines should be developed that are capable of 25 percent contingency power without damage [5]. These contingency ratings are higher than found in modern engines and would, therefore, add considerable cost to the aircraft development.

A total power failure is much less likely than a single engine failure, however, a contingency plan is still needed. For fixed-wing aircraft, a multiple engine failure is a very serious situation and generally the only option for the pilot is to attempt to glide to a safe landing area. For a total power failure in a fixed-wing commuter aircraft, the Federal Aviation Regulation (FAR) Part 23.143 only requires that the aircraft remain controllable and maneuverable during the descent so that there is a chance of finding a suitable landing area [6]. In helicopters, a complete engine failure is less serious

because of the ability to autorotate the rotors. During autorotation, a combination of forward speed and rate of descent results in an upflow that can generate thrust by “windmilling” the rotors. This thrust can be sufficient to balance the forces of gravity and maintain a constant rate of descent from which a flare maneuver can be executed to cushion the landing. In addition to requiring that rotary wing aircraft remain controllable and maneuverable in a power-off landing, FAR 29.175 also requires that Category A rotorcraft (gross weight above 20,000 lb and 10 or more passengers) must be stable in autorotation from half the maximum range glide speed to the never exceed speed.

Currently, tiltrotor aircraft fall under regulation by the Interim Airworthiness Criteria for Powered-Lift Transport Category Aircraft [7]. Although these regulations are interim, and may be expanded before a CTR is certified, they are the best indicator of likely CTR certification standards available. For a total power failure in forward flight, the interim standards have essentially the same requirements as the FARs. Without power in forward flight the tiltrotor should have little difficulty meeting these standards. The only concern is that the descent rate of a tiltrotor will be high because the wing has a higher stall speed. However, a glide landing is not the only option available as long as the aircraft has sufficient altitude. There may also be time to convert to a vertical flight mode and attempt a power-out landing. Of course, this option will only be available if the aircraft in fact does have a power-off landing capability in the helicopter configuration.

The requirements for a vertical flight mode power out situation are not clearly defined. Part XX.34 of Interim Airworthiness Criteria states the following:

The aircraft motions during and following a sudden critical propulsion system failure that is not shown to be extremely improbable shall be such that the aircraft

can be maintained within the circumscribing flight envelope and returned to the authorized flight envelope without requiring exceptional pilot skill. It shall be possible to establish a safe failure state and proceed to a landing [7].

In the FARs “extremely improbable” is generally taken to mean that less than 10^{-9} occurrences are expected per flight hour. When one considers that the flight hours of an entire fleet of multi-engine helicopters for the U.S. military is less than 10^9 flight hours, it is easy to see that a multiple engine failure cannot be shown to be extremely improbable. Certainly in the entire fleet of UH-60s, CH-46s, CH-47s, CH-53s and other multi-engine helicopters there has been at least one instance where all power to the rotor was lost. Even if advanced engines used on a CTR are more reliable than the engines of these aircraft, the drive train is more complex and at least as likely to fail. Since vertical flight is within the flight envelope of a CTR and a total power failure is very improbable, but still possible, the standards of part XX.34 apply to total power failures in a vertical flight mode. Further, in part XX.143 of the interim standards it also states that after a critical engine failure that is not shown to be extremely improbable, the aircraft “must be safely controllable and maneuverable throughout the authorized flight envelope and be adequately controllable and maneuverable within the circumscribing flight envelope” [7]. When all of these requirements are considered, the conclusion is that a CTR must be controllable and maneuverable after a total power failure at any point in the flight envelope including hover, conversion and cruise. In addition, it must be possible to reach a “safe failure state” and proceed to a landing. Unless some unconventional method of emergency power generation is designed, the ability to reach a steady autorotative state will be necessary to fulfill the controllability and “safe failure state” requirements of these regulations.

Besides some type of power failure, another safety concern for a CTR is the hazard presented by the high-speed downwash of many tiltrotor designs. The wind gusts produced by a hovering CTR could blow debris presenting a danger to ground personnel and other aircraft. The FAA may require demonstrated safe operations near the ground to protect the safety of personnel and equipment.

1.3.2 Meeting Environmental Standards

Another viability requirement is that a CTR meet environmental standards. The CTRDAC concluded that energy consumption and emissions from CTR aircraft would be slightly greater than conventional aircraft such as the Boeing 737 or the Saab 2000 turboprop [4]. However, they also recognized that these slight increases could be largely offset by reduced energy use and emissions associated with air traffic delays and ground transportation around airports. A more serious potential obstacle to a CTR is external noise. To be more convenient than other scheduled airlines, the CTR must have the use of vertiports located within population centers. In these crowded business and residential areas local governments set noise standards. The CTR noise signature must be minimized to ensure noise is not a barrier to community acceptance of vertiports. If vertiport construction was limited to less than optimal locations, it has been estimated that tiltrotor ridership could fall by as much as 30 percent [4]. To increase the likelihood of community acceptance, NASA has initiated a research and development program to achieve a 12 dB reduction in V-22 noise levels. NASA plans to meet half of this goal by managing CTR approach and departure paths and the remainder by improving rotor noise characteristics.

1.3.3 Economic Viability

Once safety and noise standards are met, a CTR design can be optimized to maximize economic viability. Factors to be considered include the costs of CTR development, production and operation. These costs in turn depend largely on the price of any new technologies that might be required to meet previously discussed safety and noise standards. Operating costs will also depend on the aircraft efficiency, payload, range and speed. Revenues will depend on the convenience and comfort of the aircraft relative to other available forms of air travel.

Research conducted over the past decade on tiltrotor commercial economics has lead to a fairly well defined aircraft size and mission profile for minimizing operating costs. Phase I of the Boeing study concluded that a large CTR able to carry 36-45 passengers over a range of at least 500 nmi would experience the most success in the commercial market [1]. For this mission, a cruise speed of around 350 knots appears to offer good balance between productivity and cost. Figure 1.1 shows that the total travel time (includes average ground time of 1 hour and 20 minutes) for a trip less than 400 miles does not decrease significantly for airspeeds above 350 mph (304 kt). Also a productivity index defined as

$$\text{Productivity Index} = \frac{\text{Payload} \cdot \text{Block Range}}{(\text{Empty Weight} + \text{Fuel Weight}) \cdot \text{Block Time}} \quad (1.1)$$

indicates that tiltrotor productivity is maximized in the range of 360 to 380 knots [8]. This index is just the mission effectiveness, or payload multiplied by block speed, normalized by mission cost represented by empty weight plus fuel weight.

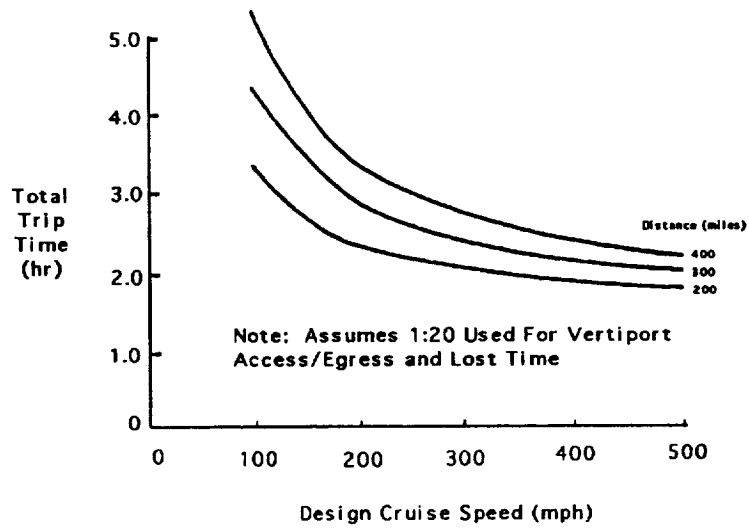


Figure 1.1: Total Trip Time vs. Design Cruise Speed [3]

Productivity is shown as a function of cruise speed in Figure 1.2.

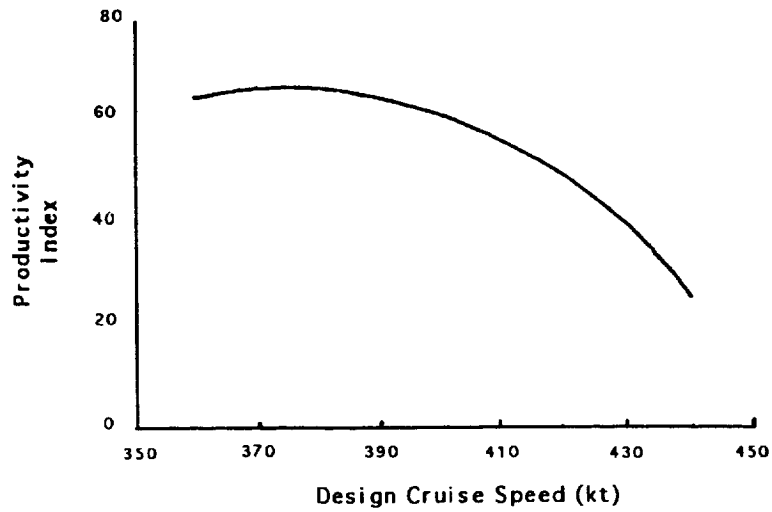


Figure 1.2: CTR Productivity Index vs. Design Cruise Speed [3]

A tiltrotor mission profile used in many studies by NASA and industry is shown in Figure 1.3. The cruise speed of 350 knots was found to minimize direct operating costs for a baseline tiltrotor aircraft [9].

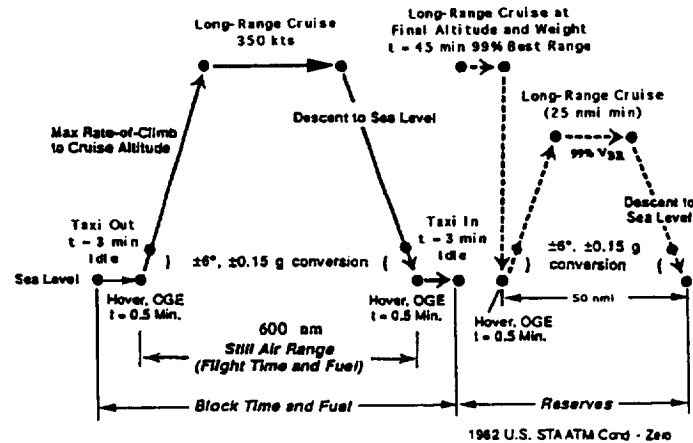


Figure 1.3: CTR Baseline Mission Profile

The mission included the fuel reserves required by federal aviation regulations for fixed-wing transport aircraft. This baseline mission is used for all aircraft sizing in this thesis.

Passenger acceptance is also obviously important to CTR viability. Potential problems in this area are the high internal noise and gust response. Without cabin acoustic treatment and improved gust response characteristics for tiltrotors, passengers will be subjected to a less comfortable ride than they are accustomed to in jetliners or turboprop aircraft. Figure 1.4 from reference [5] shows that a desirable noise level of 78 dB is far lower than found in the V-22. Design aspects that can be adjusted to affect internal noise are the amount of cabin acoustic treatment, rotor clearance from the fuselage, tip speed and number of blades. Tiltrotor gust response is likely to be high since the large, lightly-loaded rotors are more responsive to wind gusts than the

smaller and more heavily-loaded propellers of turboprops. This characteristic has been confirmed by XV-15 flight tests where a higher than normal longitudinal response to turbulence was recorded [10]. If a CTR rotor design leads to low blade loading in cruise, active controls may have to be used to provide passengers with a smooth ride.

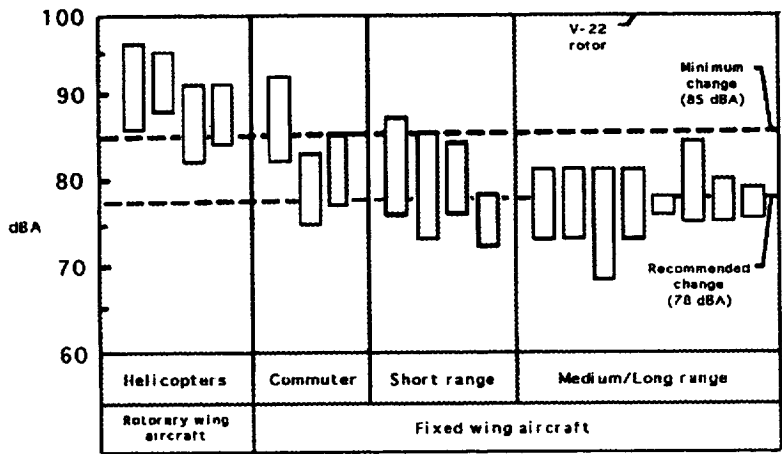


Figure 1.4: Cabin Noise Levels of Various Aircraft

1.3.4 Key Technologies for Tiltrotor Viability

Due to the civil noise, safety and economic considerations just mentioned, many of the technologies used on current military and research tiltrotor aircraft are not adequate for the civil mission. Additional research is required to develop technology needed by the CTR.

Areas of research necessary, or at least desirable for tiltrotor viability were identified by the CTRDAC and the Committee for High Speed Rotorcraft to guide the CTR development program. These committees concluded research pertaining to

meeting federal and local regulatory standards as the most critical. Low noise rotor technology and flight patterns for external noise reduction top the list. Other critical technologies identified are those needed to meet federal safety standards. These include developing designs with a capability for controlled power-out landing that meet or exceed current fixed-wing and helicopter standards and developing engine technology for higher contingency power to meet OEI flight requirements. Other suggested areas of research were ice protection, health and usage monitoring systems and cockpit design to enhance pilot situational awareness and emergency response.

Technologies that would benefit a CTR by improving performance and lowering operating costs were also recommended. While these later technologies may not represent a barrier to entering the market, they are necessary to reduce the vulnerability of a CTR to competition from conventional forms of transportation. Included in this list are improving rotor hover and cruise efficiency and reducing airframe drag. Cabin internal noise reduction and vibration suppression were recommended to improve ride quality. Structural efficiency was also deemed as enhancing to reduce the weight associated with the high wing-stiffness requirement for whirl flutter stability.

Chapter 2

The Variable-Diameter Rotor Concept

The variable-diameter tiltrotor (VDTR) shown in Fig. 2.1 has numerous advantages over conventional tiltrotor designs in both the hover and cruise flight modes. These benefits have been suggested by Fradenburgh and Matuska [11], and are presented here briefly to introduce the concepts. A more detailed explanation is given in Chapter 3.

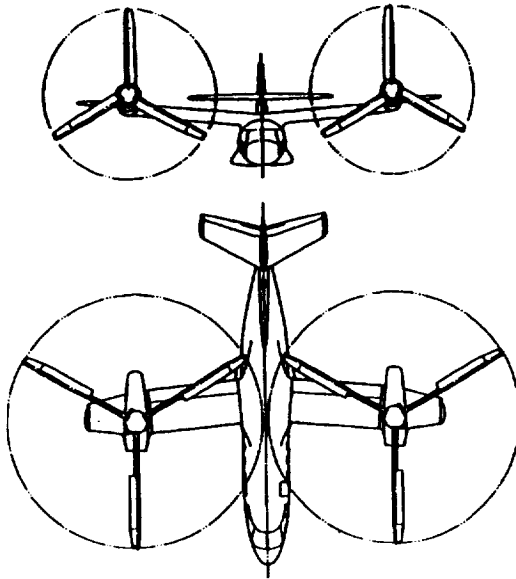


Figure 2.1: The Variable-Diameter Tiltrotor Concept [11]

Many VDTR advantages stem from the low disk loading that is possible with a large diameter rotor. Disk loading trends for various aircraft are shown in Figure 2.2.

Low disk loading tiltrotor designs will share many of the advantages of helicopters during vertical flight including low power requirements, low downwash velocities and good autorotative performance. Each of these characteristics improves tiltrotor safety. Because of a lower hover power requirement, a VDTR will require smaller engines to satisfy OEI operational requirements. This would eliminate the need to develop engines with high contingency power levels. Lower downwash velocities will reduce dangers to ground crew and other aircraft in landing areas. Low disk loading combined with high inertia rotors will reduce the autorotative rate of descent and lead to more effective flare maneuvers to give the VDTR an autorotation capability similar to helicopters. A large diameter rotor does not require a high rotor tip speeds during hover. A benefit of low tip speed and low disk loading is a reduction in blade vortex interaction (BVI) noise during descent which can be the most significant source of tiltrotor noise. Lower power requirements also permit faster and steeper takeoff profiles to reduce noise during departures.

The advantages of the VDTR during cruise are derived from the low rotor tip speeds made possible by the small diameter. Low tip speeds reduce compressibility drag and lead to higher blade loading during cruise. Both factors contribute significantly to rotor propulsive efficiency. For acceptable levels of propulsive efficiency, conventional tiltrotor aircraft must reduce tip speed during forward flight by either reducing engine RPM or using a two-speed transmission. Reducing engine speed from the design speed leads to a reduction in engine efficiency while using a two-speed transmission adds weight and complexity to the transmission. As a result of these penalties and other vibration problems, tip speed reduction is limited to about 20 percent. The VDTR avoids these penalties while using even lower, more efficient tip speeds. For the VDTR, tip speed reduction depends only on the rotor diameter

change that is possible. Other important advantages are reduced gust response due to higher blade loading and reduced internal cabin noise levels due to low tip speeds and large rotor tip distance from the fuselage.

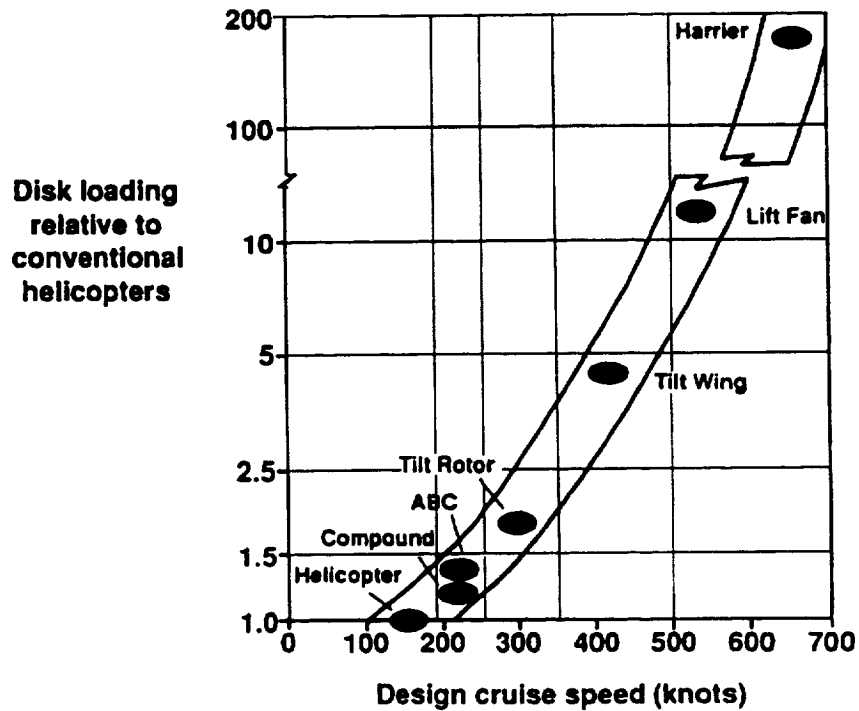


Figure 2.2: Disk Loading vs. Design Cruise Speed of Various Aircraft

2.1 Variable-Geometry Background

A variable-diameter rotor is not such a radical idea when one considers that variable geometry aircraft components are widely used in many military and civilian aircraft flying today. Notable examples are the variable sweep wings of the General

Dynamics F-111 fighter-bomber and the high lift devices used on the wings of jetliners such as the Boeing 747. In the F-111 a variable wing sweep is used to improve the take off and landing performance of the aircraft and to reduce the trade-off between range and payload. A 56 degree sweep change allows the aircraft to cruise at Mach 2.5 while still being able to land at only 110 kt in 2000 ft of runway. NASA engineers overcame stability problems associated with changing the aircraft aerodynamic center and center of mass and that plagued early experimental variable-sweep aircraft with the concept of sweeping each wing on its own pivot point rather than using a common point. Even with the added complexity of the sweep mechanism, the F-111 has proven to be one of the most reliable high-performance aircraft in the Air Force. On the Boeing 747, several variable-geometry high-lift devices are used on the wing to reduce drag in forward flight and shorten landing distances. These devices include Krueger flaps inboard of engines with variable camber slats that lie flat when retracted and adopt a cambered feature when extended [12]. Outboard of the engines, flap assemblies with three sections are found which first deflect together and then separate relative to one another at different camber angles. For both aircraft, the increased complexity of variable geometry devices is simply the price of added performance.

Variable-diameter rotors are not a new concept either. In the late 1960's a Telescoping Rotor Aircraft (TRAC) rotor system was designed and tested to explore its use for stowed rotor and compound helicopter applications. For the stowed rotor application, the advantage of the design was to alleviate dynamic and strength problems associated with stopping a rotor during flight while, for the compound helicopter, the advantage was drag reduction at high forward speeds. The TRAC rotor used a jackscrew mechanism to slide an outer blade section over an inner aerodynamically shaped tube. Wind tunnel tests and actuator mechanism cycle tests

demonstrated the performance benefits and the feasibility of the concept [13, 14]. Another variable-diameter rotor concept of the 1960's was developed specifically for tiltrotor aircraft. Rather than a jackscrew mechanism of the TRAC rotor, this design used a strap that wound or unwound around a drum attached to the drive shaft to extend or retract the blades. Another difference was that the outer blade sections of this design telescoped into the inner blade section. A 25 ft diameter version of this rotor design demonstrated 700 extensions and retractions during ground tests [15].

2.2 Possible Variable-Diameter Designs

Most of the current variable-diameter rotor research has focused on a telescoping rotor design actuated by an internal jack screw similar to the TRAC rotor system. This concept is illustrated in Figure 2.3.

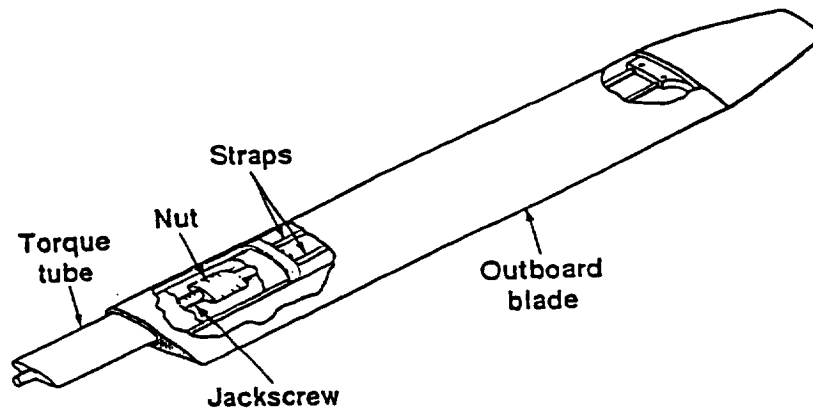


Figure 2.3: Variable-Diameter Rotor Blade [11]

The major components of the design are an outer blade section, a torque tube, a jackscrew, tension straps, and retention nuts. The function of the torque tube is to carry the blade bending moments and to transfer blade pitch control from the hub to the outer blade. The outer blade section provides the majority of the lift and slides over the torque tube during extension and retraction. The section is held by tension straps that resist the centrifugal force during rotation. The tension straps are fastened inside the outer blade section tip and run along its length into the torque tube. Inside the torque tube the straps are anchored to retention nuts threaded onto the jackscrew. When the jackscrew spins, the nuts inside the torque tube move and either extend or retract the blade. To improve the lifetime of the retraction mechanism, multiple retention nuts with few threads are used rather than a single nut with multiple threads. If only one nut were used the majority of the tensile load would be carried by the first few threads which would lead to excessive wear on the retention nuts [16]. Multiple nuts distribute the loads over more threads to reduce wear. Several tension straps are also used to make the system fail safe. Even if several straps fail the outer blade section will be retained. The jackscrew also has a tension strap in its center capable of carrying the full tensile load of the blade. If the jackscrew should break this strap would keep the blade attached.

Perhaps surprisingly, little torque from the drive shaft is necessary to extend or retract the blades. The blade extension mechanism discussed in the literature actuates the jackscrew by applying a clutch brake to an outer rotor shaft. The braking slows this outer shaft relative to the main drive shaft which, through bevel gears, causes the jackscrew to turn. Applying a brake to the upper clutch causes the jackscrew to turn in the opposite direction. A rotor hub with this clutch mechanism is shown in Figure 2.4.

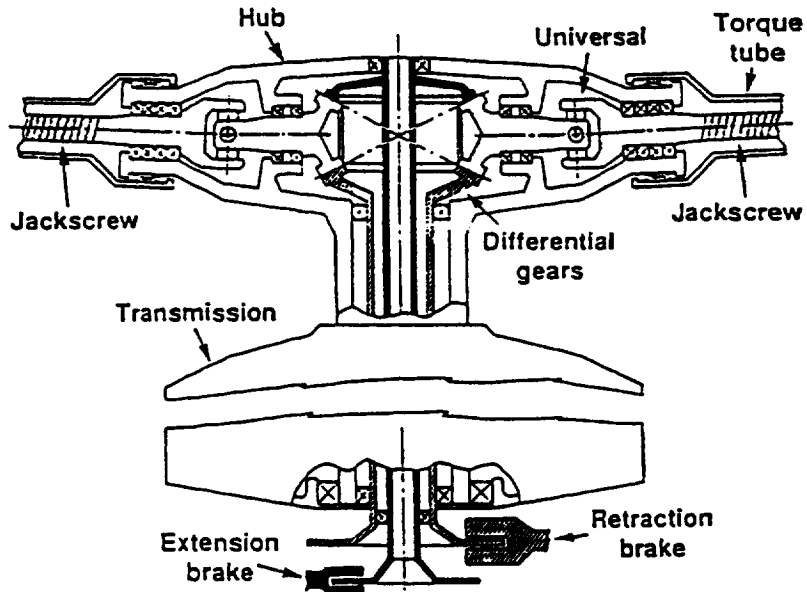


Figure 2.4: Variable-Diameter Rotor Hub Concept [11]

An important aspect of the extension and retraction process is that the rotor RPM remain constant. To maintain a constant RPM, neither angular momentum nor kinetic energy can be conserved. Figure 2.5 shows a simplified model of the variable-diameter rotor actuator mechanism. The rotor blade exists in the xy coordinate system which rotates in the XY coordinate system around point A . The mass of the outer blade is concentrated at B which rotates around A and moves relative to A in the radial direction during extension or retraction. From basic dynamics the acceleration of point B relative to point A in the nonrotating frame can be written as

$$a_B = 2\Omega \times \dot{r} + \Omega \times (\Omega \times r) \quad (2.1)$$

The first term represents the Coriolis acceleration which is tangential while the second is the centripetal acceleration in the radial direction. The tangential acceleration is in the direction of rotation during extension and opposite rotation during retraction. To produce the tangential acceleration necessary for blade retraction and extension a torque must be applied to the rotor system. The torque required does not necessarily have to come from the drive shaft. For instance, in retraction a diameter reduction at constant RPM implies that blade kinetic energy must drop. If the efficiency of the brake and differential mechanism used to retract the rotors is chosen properly, the rate of energy dissipation of this system can balance the kinetic energy drop and no external torque need be applied [11]. In extension this is not the case. For a constant RPM, tangential velocity must increase linearly with the rotor radius. Therefore, kinetic energy must be added to the system. Most if not all of the torque required could be supplied by aerodynamic forces on the blade.

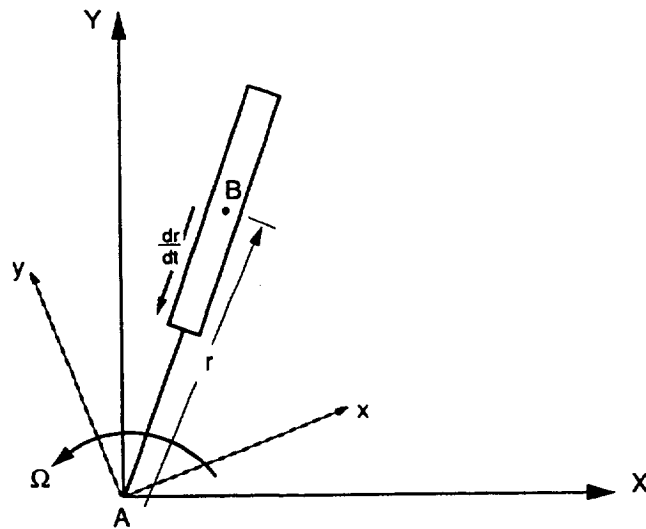


Figure 2.5: Simple Model of the Variable-Diameter Rotor

Although the jackscrew design has been studied extensively, it is not the only design to consider. The jackscrew is a heavy mechanism and the associated retention nuts will experience wear due to the high tensile loads they must bear. Mechanical tests on the jackscrew mechanism in 1976 indicated that the retention nuts could withstand 1000 retention and extension cycles with the materials available at the time [14], but a long system life may be difficult to achieve. The advantages of the jackscrew mechanism are that it is self locking and friction between the nuts and screw are available to dissipate rotor kinetic energy during retraction. Ballscrew mechanisms would eliminate wear, however, they are not self-locking. A self-locking feature may be required to maintain a constant blade diameter in the presence of unsteady aerodynamic loading. The reeled strap mechanism [15] provides an additional means for blade diameter control. Regardless of the mechanism used to actuate the blade, the basic structure of the rotor appears to be a good solution.

There are several unique aspects to the rotor design in addition to the extension and retraction mechanism. One significant feature is the large blade root cutout. Root cutout refers to the inboard portion of the blade that is not part of the airfoil. A typical helicopter root cutout is about 10 percent of the rotor radius. In the variable-diameter design the cutout could be as high as 40 percent. However, since about 90 percent of the lift in hover is produced by the outer half of the blade, the root cutout has only a small effect on rotor thrust. Furthermore, test of rotors with even 50 percent cutouts show only a small percent loss in figure of merit [17]. Another unique feature is that the outer blade section operates in compression whereas conventional blades all operate in tension. A difficult design problem is also presented by the junction between the outer blade and torque tube. This junction must bear high axial, bending and torsion loads while functioning as a joint between two different shaped blade

sections. Since the blade must slide freely over the torque tube, the blade can only have a linear twist and little if any taper. The outer blade tip is on only part of the blade that can be tapered or swept to improve aerodynamic performance.

2.3 Recent Variable-Diameter Rotor Research

A significant amount of research has already been performed on the VDTR concept including simulations, wind tunnel tests and design studies. An interactive real-time simulation of 6 VDTR configurations was performed to investigate external noise signatures and OEI Category A takeoff performance [18]. The designs were 30 passenger aircraft with a range of 600 nmi and a cruise speed of 300 kt at 25,000 ft. The acoustic analysis was performed with the ROTONET acoustic prediction system and showed that variable-diameter configurations had a significantly lower sound exposure footprint than the conventional tiltrotors designed to fly the same mission. Improved Category A takeoff performance was also predicted due to lower climb power requirements. Later, a reduced-scale wind tunnel test of a rotor designed for a 38,600 lb aircraft with a 36 passenger payload and a 600 nmi, 300 kt, at 7,500 m was performed [19]. This test used a 1/6 scale semi-span model for the purpose of demonstrating the aeroelastic performance of a VDTR during conversion, hover and cruise. This test demonstrated the feasibility of the VDTR concept with no instabilities encountered in any flight mode. Furthermore, the test verified that hover figure of merit is only degraded by a few percent by rotor root cut out (see Fig. 2.6) and that a VDTR will have improved gust response characteristics over conventional designs (see Figure. 2.7).

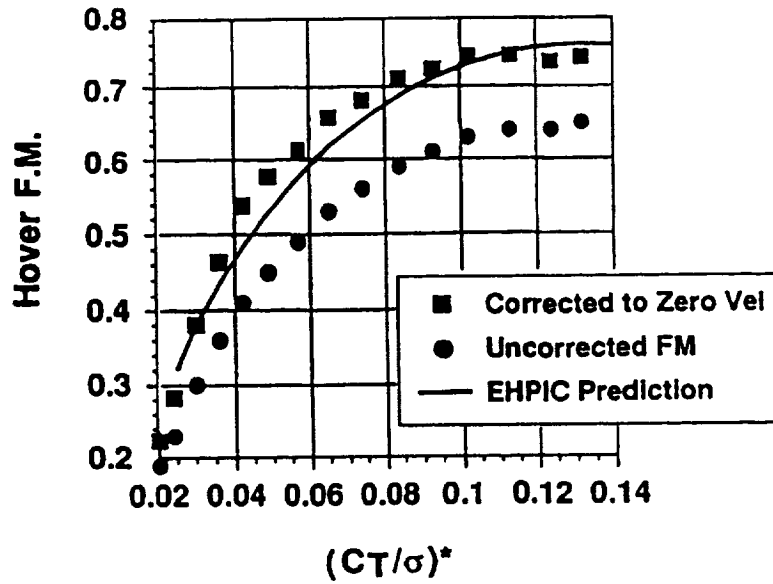


Figure: 2.6: Wind Tunnel Results for VDTR Figure of Merit [19]

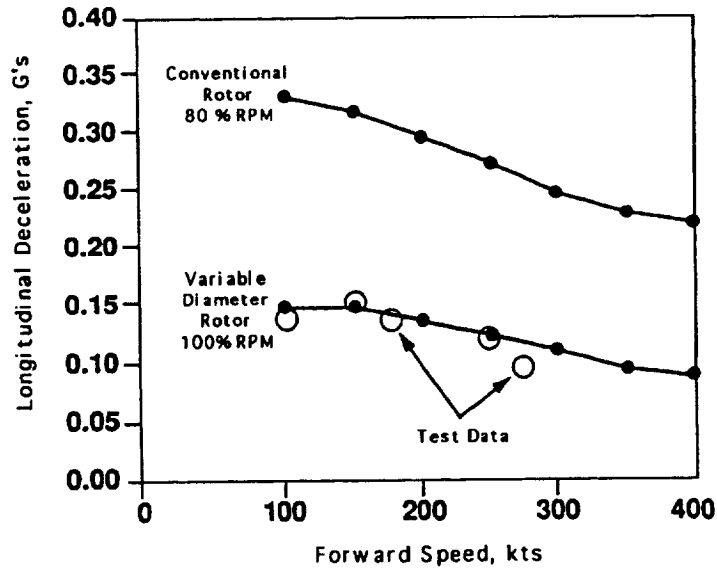


Figure: 2.7: VDTR vs. Conventional Response to a 30 fps Wind Gust [19]

The baseline VDTR design was later modified to incorporate NASA Short Haul (Civil Tiltrotor) SH(CT) guidelines which include a 40 passenger capacity, a cruise speed of 350 kt at 25,000 ft and a range of 600 nmi. New rotor designs were explored with airfoils designed specifically for tiltrotor aircraft [20]. A dual point optimizer was also developed to simultaneously optimize the rotor design for hover and cruise [21]. The dual point optimizer was created from an existing single point optimizer, the EHPIC/HERO (Evaluation of Hover-Performance using Influence Coefficients/ Helicopter Rotor Optimizer) design tool. Several designs investigated show a much higher cruise efficiency than conventional tiltrotor designs. The calculated figures of merit were only slightly lower for the VDTR than conventional designs and the corresponding hover power loading (thrust/hp) was on the order of 30 percent better for the VDTR due to its inherent lower disk loading.

2.4 Variable-Diameter Rotor Complexity

Certainly complexity is a major issue in the variable-diameter design. Increasing the complexity of any aircraft component should be avoided unless the component has a demonstrated reliability and provides a clearly needed improvement in performance. As seen in the following chapters, the variable-diameter rotor does provide a clear improvement over conventional rotors for 40 passenger civil tiltrotors.

While the reliability of a large, variable-diameter rotor has not yet been demonstrated, the concepts for the rotor and hub are no more complex than the rest of the drive system. The nacelle tilt mechanism and the interconnecting drive shaft that runs through the wings already add complexity to the tiltrotor not found in turboprops or helicopters. Testing on the TRAC rotor and model-scale tests of a variable-diameter

tiltrotor have demonstrated that the design is feasible. Another important point is that the actual diameter-change mechanism is only used for a very small portion of the flight since a typical conversion only lasts 20-40 seconds. Therefore, achieving the high reliability required of aircraft components in continual use such as the transmission or flight control system will be less difficult. While none of these facts prove that the complexity of the variable-diameter rotor is acceptable, they do indicate that it is not possible to simply disregard the concept based on the assumption that it is too complex.

Chapter 3

Advantages of a Variable-Diameter Rotor System

3.1 Introduction

A variable-diameter rotor could reduce the performance compromises inherent in tiltrotor aircraft. These compromises stem from the fact that the operating conditions of a rotor are significantly different for hover and cruise. The rotor design process must involve a dual point optimization so that a reasonable performance in both flight modes is achieved. With a fixed-geometry rotor, the majority of the parameters to be optimized such as diameter, solidity, sweep, twist and taper must remain constant for both flight modes. The rotor tip speed can vary between hover and cruise, but, for reasons to be explained later, not by much more than twenty percent. In contrast, several of the variable-diameter rotor design parameters can change between flight modes. Solidity, twist and diameter may all change within limits (solidity is defined as the ratio of the rotor blade area to the rotor disk area). The tip speed change is no longer limited to twenty percent since it changes with rotor diameter. The result is that the optimized variable-diameter design performs more like a rotor specifically designed for each flight mode. Improved areas include the hover power requirement, cruise efficiency, autorotative performance, external and internal noise levels, and gust response.

3.2 Advantages in Hover

During hover the function of a rotor is to provide a large amount of thrust to overcome the gross weight and vertical drag of an aircraft. The total power required to produce this thrust is composed of induced and profile power. Induced power represents the kinetic energy that the rotor imparts to the wake flow field per unit time. The profile power is the power required to overcome viscous drag forces that act on the rotor blades. An advantage of the variable-diameter rotor is that it requires significantly less induced power than a conventional design.

3.2.1 Induced Power

Induced power can be estimated using momentum theory. For this calculation the rotor is treated as a solid actuator disk which accelerates a mass of air downward. The rotor and airstream form a closed system over which the principles of conservation of mass, momentum and energy apply. This concept is illustrated in Figure 3.1. The thrust produced by the flowing mass of air is equal to the change in momentum imparted to the air by the rotor disk:

$$T = \dot{m}\Delta v \quad (3.1)$$

Since mass must be conserved in the closed system, the mass flow through any two points must be constant. Thus, the mass flow between locations **0** and **2** is equivalent to the flow past **1** or

$$\dot{m} = \rho A v_1 \quad (3.2)$$

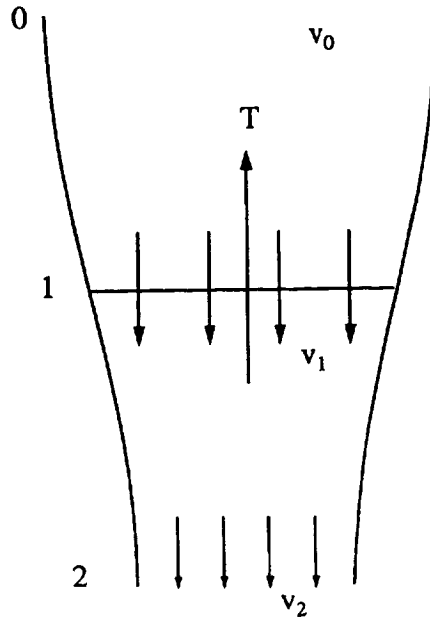


Figure 3.1: Momentum Theory Control Volume

In hover the air far above the rotor has zero velocity so the change in velocity over the system is

$$\Delta v = (v_2 - v_0) = v_2 \quad (3.3)$$

Combining these equations the rotor thrust becomes

$$T = \rho A v_1 v_2 \quad (3.4)$$

The velocities v_1 and v_2 may be related by applying the conservation of energy between locations 1 and 2. The work done per unit time by the rotor is equivalent to the change in kinetic energy per unit time imparted to the slipstream or

$$Tv_1 = \frac{1}{2} \dot{m}v_2^2 \quad (3.5)$$

Combining Eq. 3.2, Eq. 3.4 and Eq. 3.5 the relationship between the velocities at locations 1 and 2 becomes

$$v_2 = 2v_1 \quad (3.6)$$

From this relationship the thrust can be rewritten as

$$T = 2\rho Av_1^2 \quad (3.7)$$

Note that v_1 is the velocity imparted to the wake flow field by the rotor disk, and it is called the induced velocity. From Eq. 3.7 the induced velocity can be written as

$$v_i = \sqrt{\frac{T}{2\rho A}} \quad (3.8)$$

The induced power is just the thrust times the induced velocity or

$$P_i = T \sqrt{\frac{D.L.}{2\rho}} \quad (3.9)$$

where D.L. is the disk loading defined as

$$D.L. = \sqrt{\frac{T}{A}} \quad (3.10)$$

In the following discussion it is convenient to use standard nondimensional forms of the thrust, torque and power. Therefore the following coefficients are defined:

$$C_T = \frac{T}{\rho\pi R^2(\Omega R)^2} \quad (3.11)$$

$$C_Q = \frac{Q}{\rho\pi R^2(\Omega R)^2 R} \quad (3.12)$$

$$C_P = \frac{P}{\rho\pi R^2(\Omega R)^3} \quad (3.13)$$

Since $P = Q\Omega$ the torque and power coefficients are equivalent.

The induced power calculated from momentum theory can be rewritten with these coefficients as

$$C_R = \frac{C_T^{3/2}}{\sqrt{2}} \quad (3.14)$$

The power calculated here is less than the actual induced power due to losses neglected in momentum theory. These include non-uniform inflow to the rotor, rotation of the

wake and losses at the blade tips. The induced power calculated from momentum theory is also known as the ideal power. It is ideal in that all losses have been ignored. Typically, for a helicopter, the actual induced power is 10-20 percent more than the ideal power [22]. The true induced power can be written as

$$C_{P_i} = \kappa \frac{C_T^{3/2}}{\sqrt{2}} \quad (3.15)$$

where κ is some empirically determined correction factor.

From Eq. 3.9 it is seen that the induced power is set by the hover disk loading of the rotors. For a tiltrotor in hover, the disk loading is defined by Eq. 3.10 where T is half of the aircraft gross weight. Variable-diameter designs are capable of a low disk loading because they have a large rotor diameter in hover. As seen in Fig. 3.2, the maximum diameter of a conventional rotor is set by the requirement to clear the fuselage by a safe distance.

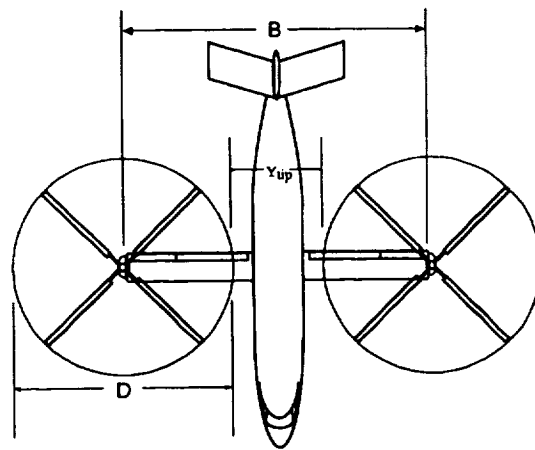


Figure 3.2: Conventional Tiltrotor Tip Clearance

In contrast, a safe rotor-fuselage clearance is maintained for the variable-diameter design because the rotor diameter decreases during the conversion to forward flight. As illustrated in Fig. 3.3, the only requirement on the hover diameter is that the rotors clear one another by some safe distance.

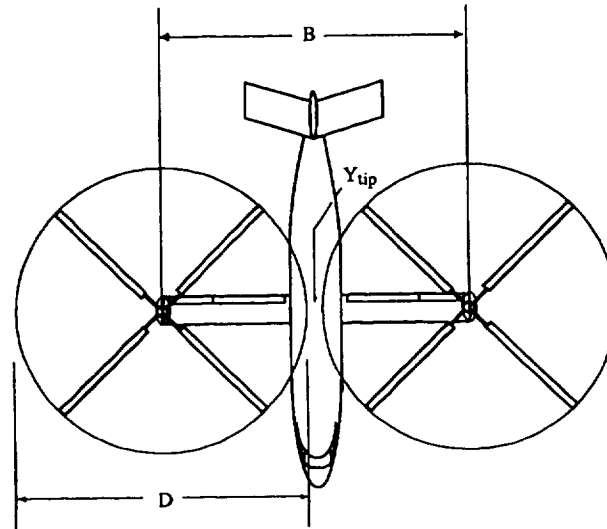


Figure 3.3: Variable-Diameter Tiltrotor Tip Clearance

The difference in disk loading and required power is significant, particularly for a forty-passenger size tiltrotor. For example, with a rotor tip clearance of 2 ft, a fuselage diameter of 9 ft and a 54 ft wing span, a conventional rotor could have a diameter of 41 feet. For the same aircraft dimensions with a 1 ft. clearance between rotor tips, the variable-diameter rotor could have a diameter of 53 feet. If the gross weight of both aircraft were about 45,000 lbs, the disk loading of the variable-diameter design would be about 10 psf compared to 17 psf for the conventional design. From Eq. 3.9, the corresponding ideal power requirement for each conventional rotor would be 2450 hp compared to only 1900 hp for each variable-diameter rotor. The 12 ft

increase in diameter would therefore lead to a 30 percent decrease in ideal power for the same rotor thrust.

3.2.2 Figure of Merit

The profile power and all other power losses ignored in momentum theory are accounted for by a factor known as the figure of merit. The hover figure of merit is a measure of rotor hover efficiency. It is defined as the ratio of the minimum power for which the helicopter could hover to the actual power required to hover. Therefore, the figure of merit is the ratio of the ideal power calculated from momentum theory to the actual power required after all losses are included. By combining Eq. 3.9 and Eq. 3.10 to form the induced power, the figure of merit can be expressed as

$$\text{F.M.} = \frac{T^{1/2}}{P\sqrt{2\rho A}} \quad (3.16)$$

where P is the actual power required. A dimensionless form of this expression can be written using the coefficients defined in Eq. 3.11-3.13:

$$\text{F.M.} = \frac{C_T^{1/2}}{\sqrt{2}C_Q} \quad (3.17)$$

where

$$C_Q = \kappa \frac{C_T^{3/2}}{\sqrt{2}} + C_{Q_0} \quad (3.18)$$

The term C_{Q_0} represents the profile torque (or power) required to drag the rotors through the viscous atmosphere.

For a given thrust requirement in hover (gross weight + download) and a given rotor diameter, the figure of merit depends on induced losses and on the profile drag of the rotor blades. The sources of induced loss have already been discussed. Skin friction, flow separation and compressibility effects all contribute to the profile drag. The torque required to overcome this drag can be substantial, particularly when the inboard portion of the rotor operates above its stall angle of attack or when the blade tips operate above their drag divergence speed. All of the losses at the rotor depend on the details of the actual rotor design such as solidity, twist, taper and tip speed.

To see how blade design affects figure of merit consider the forces acting on an airfoil cross-section as depicted in Figure 3.4.

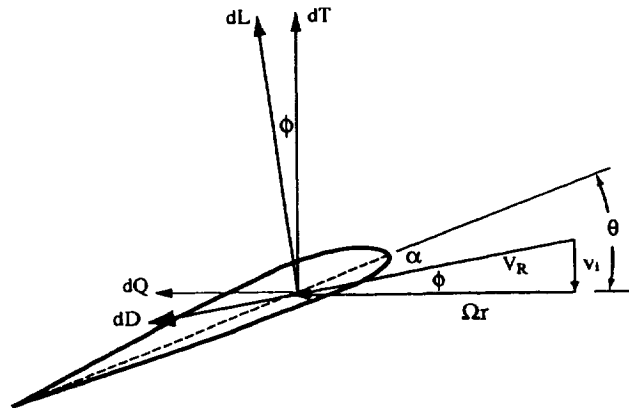


Figure 3.4: Forces Acting on an Airfoil During Hover

The incremental lift and drag produced by this airfoil is given by

$$dL = \frac{1}{2} c_l \rho V_R^2 c dr \quad (3.18)$$

$$dD = \frac{1}{2} c_d \rho V_R^2 c dr \quad (3.19)$$

where c is the element chord length, V_R is the inflow velocity and c_l is the element lift coefficient defined as

$$c_l = a(\theta - \phi) \quad (3.20)$$

Here a is the lift curve slope of the airfoil. Since the induced velocity (v_i) is much smaller than the tangential velocity (Ωr), the following assumptions are justified:

$$V_R \approx \Omega r, \quad (3.21)$$

$$\cos \phi \approx 1, \quad (3.22)$$

$$\sin \phi \approx \phi, \quad (3.23)$$

$$\phi = \frac{v_i}{\Omega r} \quad (3.24)$$

Based on these assumptions the differential thrust and torque acting on the airfoil are

$$dT = \frac{1}{2} \rho c_l (\Omega r)^2 c dr \quad (3.25)$$

$$dQ = \frac{1}{2} \rho c (\Omega r)^2 (c_l \phi + c_d) r dr \quad (3.26)$$

The total thrust and torque are determined by integrating these equations along the length of each rotor blade. The integration is difficult because the chord, inflow angle and lift and drag coefficients are all functions of radius. Even without performing the integration the equations illustrate the key factors affecting figure of merit. These are the chord distribution along the blade, the lift curve slope and drag of the airfoils and the blade angle of attack at each radial station.

Care must be taken when comparing the figure of merit directly for conventional and variable-diameter tiltrotors. This is because for both designs rotor design parameters can not be chosen freely due to cruise performance considerations. The figure of merit can vary widely depending on the amount that propulsive efficiency is compromised. The variable-diameter rotor figure of merit is penalized by the presence of the torque tube spar and the linear twist constraint. The spar cross-section has a symmetric airfoil shape which must have a relatively high thickness to chord ratio for structural reasons. In hover, the linear twist requirement leads to high angles of attack on outer portion of this spar which cause the spar to stall. The corresponding rise in profile drag and loss in lift will reduce the thrust and increase the profile torque of the rotor. The overall impact on figure of merit is diminished to some extent by the fact that the spar has a lower chord and corresponding area and thus produces less drag when stalled. In general, the figure of merit of a variable-diameter rotor will be slightly lower than that of a conventional rotor while the opposite is true for the propulsive efficiency. This trend can be seen in Fig. 3.5 which is based on data generated from an EHPIC/HERO analysis presented in reference [21].

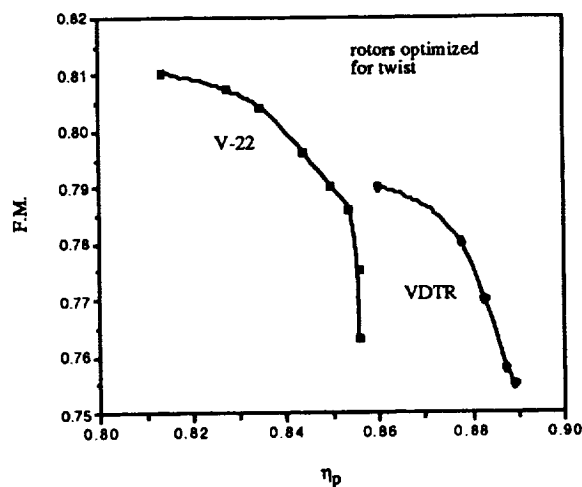


Figure 3.5: Figure of Merit vs. Propulsive Efficiency Trend

3.2.3 Rotor-Airframe Interactions

Interactions between the rotor wake and the airframe can have a significant effect on the hover power requirement. For a tiltrotor, important interactions take place between the wing, fuselage and rotor. As the rotor wake impinges on the wing a download is produced by drag forces on the wing and a change in momentum of the rotor wake. The effect of this download is to increase the gross weight of the aircraft that must be lifted in hover. In addition to producing download, the presence of the wing and fuselage causes a recirculation of the rotor wake which can increase the induced power. Once some forward speed is achieved, however, the benefits of side by side rotors will reduce the power requirements. For all of these reasons, the difference in download between a conventional rotor and a variable-diameter rotor is difficult to quantify.

A critical factor in the download is the ratio of the equivalent flat plate area washed by the rotor wake to the disk area of the rotor. This fact can be shown

following a short discussion by McCormick [23]. Equivalent flat plate area is a relative measure of drag defined as

$$f_v = \frac{D_v}{q} \quad (3.27)$$

where D_v is the vertical drag force and q is the dynamic pressure in the wake. In this case, f_v is an area with a $C_D = 1$ that produces the same vertical drag as the actual wing. Assuming the rotor wake is fully developed and uniform, the download can be written as

$$D_v = f_v \frac{T}{A} \quad (3.28)$$

since from Eq. 3.6 and 3.8 $q = T/A$. The total thrust required in hover is the aircraft gross weight plus the download which is

$$T = \frac{W}{1 - \left(\frac{f_v}{A}\right)} \quad (3.29)$$

Based on this analysis, a low download would be expected of a variable-diameter rotor due to the large disk area. The increase in disk area should be greater than the increase in equivalent flat plate area since the flat plate area varies with R , and the disk loading varies with R^2 .

Due to the complex nature of tiltrotor download the preceding analysis may be an oversimplification. In actuality the equivalent flat plate area depends on more than just

the wing area washed by the rotor wake. The velocity in the wake is distributed unevenly because of the high twist required in tiltrotor blade designs. Also, flow patterns due to the presence of the fuselage keep much of the wake from simply flowing past the wing and causing drag.

Tests of a 2/3 scale V-22 rotor, wing and image plane described in Ref. [24] have shown that download in tiltrotors is due to both chordwise and spanwise flow along the wing. The chordwise flow occurs near the wing tip while the spanwise flow is found on the inboard wing sections. The chordwise flow falls off of the wings at the trailing edge and causes a drag force on the wing. This force can be calculated by dividing the wing into N panels and adding the contribution of each panel. By this method the download from the chordwise flow is equivalent to

$$D_v = C_D \sum_{i=1}^N A_i q_i \quad (3.30)$$

where A_i and q_i are the area and dynamic pressure of the wake acting on the i th panel of the wing in the chordwise flow region. A typical drag coefficient for a wing section at 90 degrees incidence is about 1.4 [25]. In contrast, the spanwise flow does not fall off the wing. The majority of this flow travels along the wing toward the fuselage where it meets the flow from the other rotor. When the flows from the two rotors meet at the aircraft plane of symmetry, they interact with the fuselage. The fuselage prevents the flow from spreading equally in all directions in the image plane and creates a fountain that flows upwards, back towards the rotors. This is commonly referred to as the fountain effect. The download caused by the spanwise flow as it is turned by the wings and image plane is equivalent to the total change in momentum of

the flow as it is turned 180 degrees. If little or no losses are assumed to occur as the flow is turned, the change in momentum is equivalent to the original momentum flux in the wake. This flux is simply

$$D_{v_s} = q_s A_s \quad (3.31)$$

where q_s and A_s are the average dynamic pressure and the area of the wake involved in the spanwise flow.

Predicting the relative download of variable-diameter and conventional rotors based on this model is difficult. The relative size of the rotor wake producing chordwise and spanwise flow was found to vary with rotor operating conditions and it is also expected to vary with different aircraft configurations [24]. In addition, download was found to increase with C_T as the highest velocity portion of the wake shifted into the spanwise flow region. This trend is shown in Fig. 3.6.

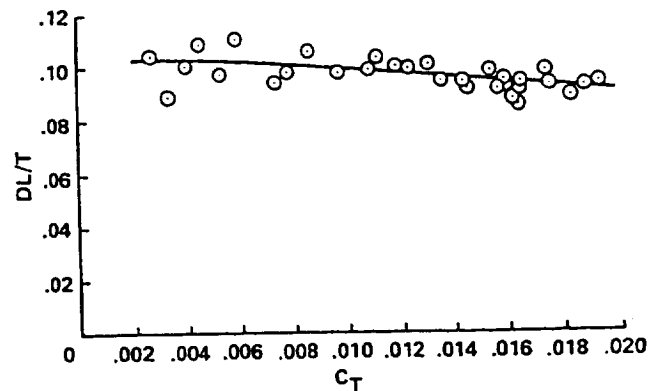


Figure 3.6: Download vs. C_T for a V-22 Tiltrotor [24]

A low disk loading variable-diameter rotor will have a lower induced velocity and this velocity will be distributed on the outer part of the rotor for a range of operating conditions. These factors would indicate a decrease in download due to a lower momentum flux in the wake and a concentration of the high-velocity wake in the spanwise flow region. However, the effect a variable-diameter design will have on the relative size of the spanwise and chordwise flow region is unknown. Another unknown is the effect decreased rotor spacing would have on the induced power during hover. In the large-scale model tests of the V-22, the presence of a standing vortex in the corner of the wing and image plane, similar to a vortex ring, was found to decrease rotor thrust by about 1.6 percent [24]. This effect was largely balanced by the benefit of the wing which acted as a partial ground plane and reduced the induced power. Since the wake of the variable-diameter rotor will extend further inboard on the wings and will have a lower velocity than the wake of a conventional design, the fountain may be diminished and the induced power penalty would likely be less. In a low-speed hover mode, the variable-diameter design will also experience a reduction in induced power due to a positive interference between the closely spaced rotors. Figure 3.7 shows this power reduction as a function of lateral shaft spacing. Experimental data plotted in this figure show that induced power is reduced by approximately 22 percent for a lateral shaft spacing of 2.05 rotor radii. The positive interference disappears as shaft spacing approaches 2.5 radii. The other factor involved in the interference is forward speed. For a shaft spacing between 2.0 and 2.5 radii, the maximum reduction in power is experienced at an advance ratio of 0.09, where the advance ratio is defined as

$$\mu = \frac{V}{V_{tip}} \quad (3.32)$$

At zero forward speed the benefits disappear as they do for advance ratios above about 0.20 [26]. Since the variable-diameter rotor concept will likely have a shaft spacing of about 2.05 radii, the induced power should be reduced while operating at low-speeds in the hover mode. This power reduction will be particularly helpful during OEI scenarios while the pilot maneuvers the aircraft to find a suitable landing area. A typical conventional design will have a shaft spacing near or above 2.5 radii where little or no interference effects are experienced.

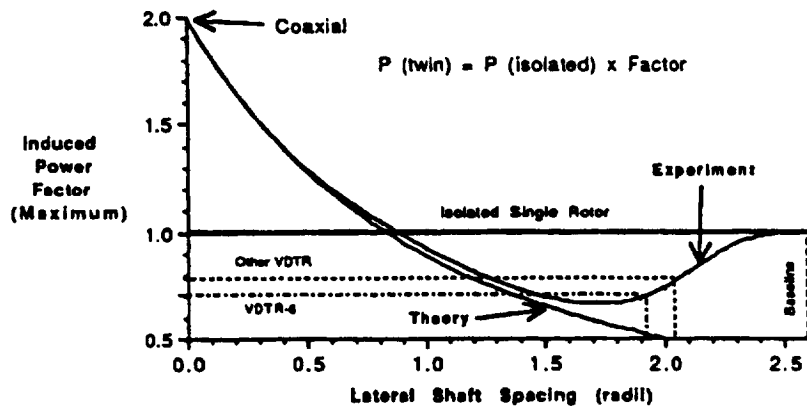


Figure 3.7: Beneficial Interference Effects for Low Rotor Shaft Spacing [26]

Considering all the factors that influence download in tiltrotors, it is difficult to quantify the net impact rotor and wing interactions would have on variable-diameter hover power. There are several potential benefits. Further testing is required to quantify the anticipated download reduction.

3.2.4 Summary of Hover Benefits

Clearly the variable-diameter design represents a large improvement in hover performance over a higher disk loading conventional design. The significantly lower induced power more than compensates for any differences that may exist in figure of merit. The download is also expected to be less. As a result of these benefits, the hover power requirement may be as much as 30 percent lower for the VDTR. The power reduction translates into more payload for a given engine size or a reduction in engine size for the same payload.

3.3 Advantages During Cruise

The variable-diameter rotor also has an advantage over conventional designs during cruise because of higher rotor propulsive efficiency and reduced gust response. A higher propulsive efficiency reduces fuel consumption, and a reduced gust response improves passenger comfort. Both advantages are attributable to a higher blade loading of the variable-diameter rotor in cruise.

3.3.1 Rotor Propulsive Efficiency

Propulsive efficiency is the ratio of the useful power to the power input from the drive shaft. The useful power is simply the power required to produce a certain thrust at a given flight speed. Written mathematically propulsive efficiency is

$$\eta_p = \frac{TV}{P} \quad (3.33)$$

where P is the total power input and TV is the useful power. This equation can also be written in terms of the nondimensional coefficients defined in Eq. 3.11 - 3.13 (recall $C_Q = C_p$):

$$\eta_p = \mu \frac{C_T}{C_Q} \quad (3.34)$$

where μ is an advance ratio defined in Equation 3.32. To understand the forces that affect efficiency, consider two blade elements operating with high and low RPM as shown in Figure 3.8. The forces acting on these elements in the thrust and torque direction can be expressed as

$$dT = dL \cos \phi - dD \sin \phi \quad (3.35)$$

and

$$dQ = dL \sin \phi + dD \cos \phi \quad (3.36)$$

where

$$\cos \phi = \frac{\Omega r}{V_R}, \quad \sin \phi = \frac{V + v_i}{V_R} \quad (3.37)$$

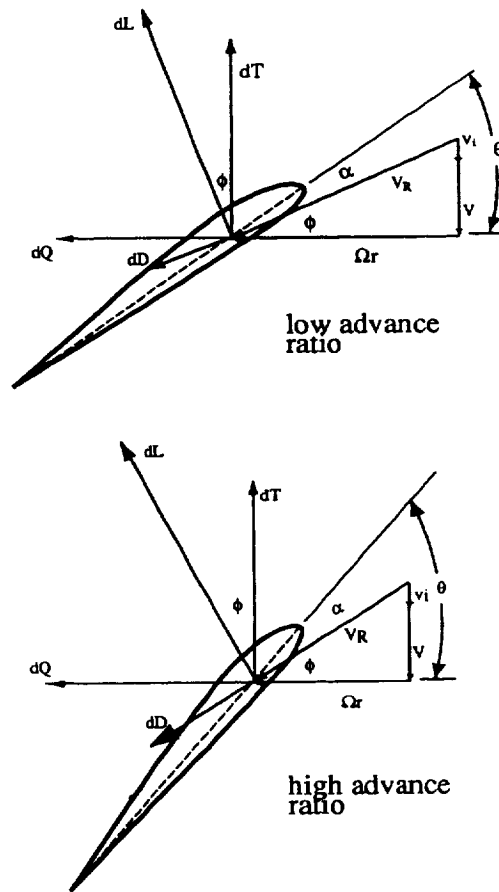


Figure 3.8: Forces Acting on Airfoils in the Cruise Flight Mode

If the very small induced velocity (v_i) is ignored, the airfoil efficiency can be written as

$$\eta_p = \frac{dT}{dQ} \tan \phi \quad (3.38)$$

From this equation it is evident that the factors affecting propulsive efficiency are the inflow and the integrated lift and drag across the rotor blades.

With a conventional rotor, the blade area and tip speed required for hover are too

high for the rotor to operate at its best efficiency in forward flight. This design compromise is a result of the cruise thrust requirement being only about ten percent of the hover value. To provide such a small thrust without a corresponding drop in tip speed or blade area, the blades have to operate at a low thrust coefficient to solidity ratio. This ratio is really just a thrust coefficient referenced to blade area rather than disk area and is defined as

$$\frac{C_T}{\sigma} = \frac{T}{\rho A_b (\Omega R)^2} \quad (3.39)$$

For reasons to be explained shortly, in a lightly loaded condition (low C_T/σ) the rotor has a low thrust to torque ratio and thus, a low propulsive efficiency. An equally important reason for tip speed reduction is that drag due to air compressibility is more significant with high tip speeds. In cruise the rotor blade sections actually follow a helical path defined by the vector addition of the flight velocity and their own rotational speed. On the outer portion of the blade the combination of these velocities leads to high tip Mach numbers and an associated rise in drag which also reduces the rotor thrust to torque ratio. This is commonly referred to as drag divergence.

To improve cruise efficiency, conventional tiltrotors reduce tip speed from the hover value by reducing rotor RPM by about 10 percent. Higher efficiency is possible because of reduced compressibility drag and a higher rotor C_T/σ .

The increase in rotor profile torque due to compressibility effects can be calculated from an experimentally determined compressibility drag factor. This factor can be expressed as a function of the difference in the helical Mach number, ($M_{.75}$) and

the drag divergence Mach number (M_{DD}) at the rotor 75 percent radius [27]:

$$f_c = \begin{cases} 1 + 42.51(M_{.75} - M_{DD})^2 + 3476(M_{.75} - M_{DD})^4, & M_{DD} > M_{.75} \\ 1, & M_{DD} \leq M_{.75} \end{cases} \quad (3.40)$$

where

$$M_{.75} = M \sqrt{1 + \frac{9}{16\mu}} \quad (3.41)$$

To account for compressibility effects, the rotor subsonic profile torque is simply multiplied by f_c . Figure 3.9 shows the compressibility factor as a function of tip speed. This curve is based on an example 41 ft rotor operating with a forward speed of 350 kt at 25,000 ft.

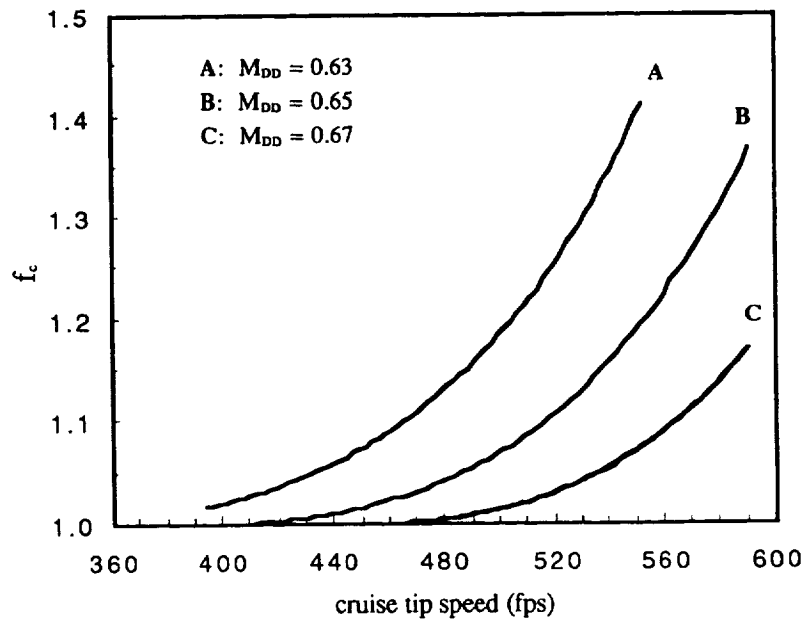


Figure 3.9: Rotor Compressibility Drag Factor

The relationship between tip speed, C_T/σ and propulsive efficiency is less obvious. This is because if thrust is held constant and tip speed is reduced, μ , C_T/σ and C_Q/σ all increase. The efficiency could increase or decrease depending on the relative magnitudes of these changes. A simple momentum theory can be used to show that η_p does indeed increase as C_T/σ increases with tip speed. This theory, developed by Schoen and McVeigh of Boeing Helicopters, has been shown to agree closely with experimental data on tiltrotor cruise efficiency [27]. The total torque coefficient acting on the rotor blade can be defined as

$$C_Q = C_{Q_{\text{profile}}} + \mu C_T + \frac{C_T^2}{2\mu} \quad (3.42)$$

where

$$C_{Q_{\text{profile}}} = f_c C_{Q_0} \left[\left(1 + \frac{5}{2} \mu^2 \right) \sqrt{1 + \mu^2} + \frac{3}{2} \mu^4 \ln \left(\frac{1 + \sqrt{1 + \mu^2}}{\mu} \right) \right] \quad (3.43)$$

The coefficient C_{Q_0} is the rotor profile torque coefficient in hover which can be determined experimentally. The compressibility drag scaling factor (f_c) was defined in Equation 3.40. These equations were used to generate the following plots for the example 41 ft rotor which has a solidity of 0.144. Figure 3.10 shows the increase in propulsive efficiency with C_T/σ for a fixed tip speed. This is the well known increase in efficiency due to increased blade loading (increased thrust). Similarly, Fig. 3.11

shows the change in η_p with C_T/σ at a constant thrust.

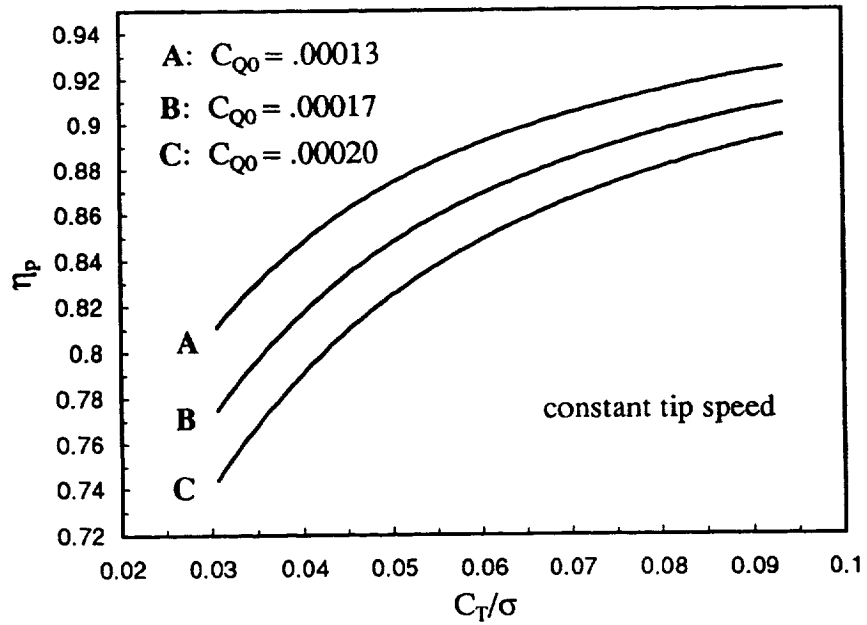


Figure 3.10: η_p vs. C_T/σ for a Constant Tip Speed

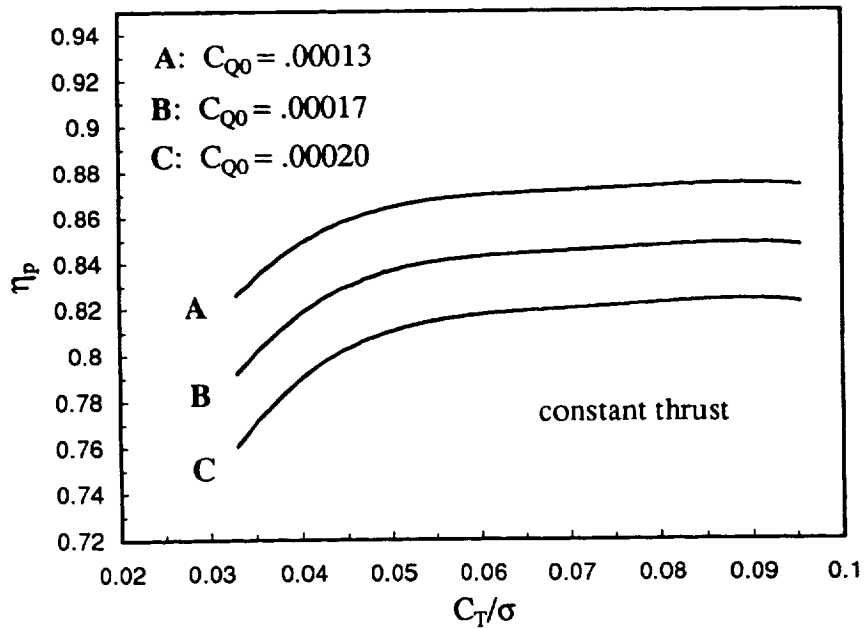


Figure 3.11: η_p vs. C_T/σ at Constant Thrust

In this case the efficiency increase is solely due to decrease in tip speed. In the former case efficiency increases because C_T increases faster than C_Q . In the latter case C_Q actually increases faster than C_T because the higher inflow tilts the lift vector in the torque direction. The efficiency only increases because the growth of μ outpaces the decrease in C_T/C_Q . So, although the in-plane components of the lift and drag acting on the rotor increase, a reduction in ΩR reduces the power requirement.

For a fixed geometry rotor, the only way to reduce the tip speed is to reduce rotor RPM. This can be accomplished through the transmission or by reducing engine turbine speed. Both methods have limitations and associated penalties. Drive system weight is increased if the transmission must perform the RPM reduction. On the other hand, reducing the turbine speed reduces engine efficiency. Typical engines have a quadratic drop-off in power as turbine speed is varied from the optimum. In practice it appears that due to vibration problems, the ratio of cruise tip speed to hover tip speed can not be much less than 0.84 which is the V-22 value.

Reducing tip speed by varying rotor diameter is a much better way to increase C_T/σ . One reason is that C_T/σ varies faster with R than with Ω since

$$\frac{C_T}{\sigma} \propto \frac{T}{(\Omega R)^2 R} \quad (3.44)$$

At the same time a diameter change avoids the engine efficiency reduction associated with an RPM reduction. The amount of tip speed reduction is also less limited since it depends on the amount of diameter change possible rather than the RPM reduction

possible. Diameter reductions corresponding to a tip speed ratio of 0.66 have been demonstrated in scaled model testing [13, 19].

With either rotor type, proper blade design choices must be made in conjunction with tip speed reduction to ensure high efficiency. Returning to the blade element pictures in Fig. 3.8, it is seen that increasing the advance ratio by a tip speed reduction tilts the lift vector in the torque direction. To avoid the associated efficiency penalties, blade area and twist must be chosen so that the blade spanwise loading distribution minimizes the amount of torque due to lift. As pointed out by Dadone, Liu, Wilkerson and Acree in high-speed-proprotor studies, simply designing the blades to operate at maximum L/D does not suffice [28].

The tiltrotor blade twist distribution is a compromise between hover and cruise requirements. In cruise, the inboard portions of the blade should be highly twisted in order to avoid large negative angles of attack. This is in conflict with the hover requirement. In hover a high inboard twist will cause these sections to stall, reducing figure of merit. For a variable-diameter rotor, compromises in blade twist are not as significant. The inboard portion of this rotor consists of the torque tube which has a small area and produces less drag when stalled in hover. Also, this rotor operates at higher advance ratios in cruise so the differences in inflow along the length of the blades are not as pronounced and less blade twist is required. A simple linear twist on the outer blade section, which works well in hover, is also adequate for cruise.

Although the cruise efficiencies of conventional rotors are not poor, they are not as high as is possible with a variable-diameter rotor. Limits on RPM reduction and associated penalties prevent a conventional rotor from operating in a C_T/σ range that corresponds to the highest efficiencies. In contrast the variable-diameter rotor is

capable of operating at a much higher C_T/σ without any reduction in engine efficiency. Studies indicate that a 7 percent increase in propulsive efficiency over current tiltrotor levels should be possible [11].

3.3.2 Gust Response

An aircraft response to wind gusts is largely determined by wing loading, and for propeller aircraft also blade loading. The high wing loading of tiltrotor aircraft should minimize response to vertical gusts, however, horizontal gusts may cause an unacceptable longitudinal motion depending on rotor size and blade loading. Conventional designs have large, lightly loaded rotors in cruise and will have a higher response than found in modern turboprops. Evidence of increased gust response was observed in XV-15 flight tests where the aircraft was found to experience a longitudinal chugging motion in response to moderate air turbulence [10]. Since the variable-diameter rotor is smaller and more highly loaded in cruise, its gust response should be closer to the level of modern turboprops. As seen in Fig. 2.7 which shows the response of a scaled model to a simulated 30 fps horizontal gust, the response of a variable-diameter rotor is significantly less than that predicted for a larger, conventional rotor.

3.4 Improved Autorotation Capability

Autorotation could be used in tiltrotor aircraft, as it is for helicopters, to provide for a safe, controlled landing in the event of a total power failure. Many conventional

designs, however, may have only a limited ability to autorotate. Highly twisted blade sections found on conventional tiltrotors resist rotor autorotative forces. High disk loading leads to a high rate of descent once a steady autorotative state has been established. Smaller rotors also have less inertia available to store the kinetic energy of the falling aircraft in order to arrest the vehicle's descent. The variable-diameter design, with its higher inertia, lower twist and lower disk loading promises to have a significantly improved autorotative capability over a much larger range of flight conditions.

Autorotation is a condition where a rotor is driven by aerodynamic forces without any torque from the drive shaft. The forces required are generated by an upward flow of air through the rotor disk as the aircraft descends. Because of the upward flow, the lift vector is tilted forward and has a component in the plane of rotation. This condition is seen in Figure 3.12.

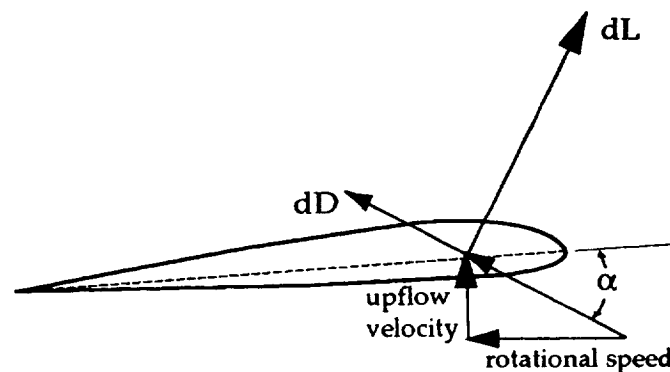


Figure 3.12: Forces Acting on an Airfoil During Autorotation

If the lift component in the rotor plane is enough to overcome the profile drag of the rotor section, it will drive the section forward. In this case the rotor is said to autorotate.

The phenomena of autorotation can be used by a skilled pilot in a well designed aircraft for emergency power-out landings. Immediately following a total power failure, engine drive trains are designed to disengage from the rotor so it is free to rotate. The pilot must react within a few seconds to prevent rotor rpm decay. The first task is to reduce the rotor collective pitch to minimize the resistance to rotor rotation. Next, the pilot gradually adjusts the rotor cyclic pitch to achieve a forward speed that corresponds to the minimum power requirement. If the rotor is designed properly, at some achievable rate of descent, the upflow through the rotor will generate enough aerodynamic torque to enable the rotors to produce a substantial amount of thrust. When this thrust is sufficient to balance the forces acting on the aircraft, a steady rate of descent will be achieved. Once established, the descent at constant speed continues until the aircraft is within a few hundred feet of the ground. At this altitude the pilot begins a flare maneuver to minimize the touchdown speed and arrest the rate of descent to a level that can be sustained by the landing gear. During a landing flare, the pilot tilts the rotors to the rear, thereby creating a large upflow through the disk. This maneuver transfers much of the aircraft kinetic energy to the rotor resulting in a decreased forward speed and rate of descent. Before the tail impacts the ground, the pilot levels the aircraft and adjusts the blade pitch to create thrust from the kinetic energy that has been stored the rotor blades. If the rate of descent was not too great, the thrust produced during the flare maneuver will be sufficient to ease the aircraft to the ground.

The important factors in an autorotative landing are the height and velocity at the time of engine failure, the torque and thrust available from the rotor during autorotation, the magnitude of the steady rate of descent that is achieved and the amount of kinetic energy that can be stored in the rotor during the flare maneuver.

For tiltrotors, the effect of the wings is also important. No tests of rotor-wing interaction during autorotation in tiltrotors have been published, however, for winged helicopters it is desirable to unload the wings during autorotation by keeping the airframe in a nose down attitude. The lift lost is of no consequence because the low disk loading rotor can easily produce the thrust required to enter a steady autorotative state. Since the wings are parallel with the flow, their disruptive effect is minimized. Unlike the helicopter, however, the smaller rotors of a conventional tiltrotor may not be able to provide the thrust necessary for a steady autorotative state, and the wings will have to carry some load. If this is the case, autorotation will also depend on the complex aerodynamic interaction of the rotors and wings.

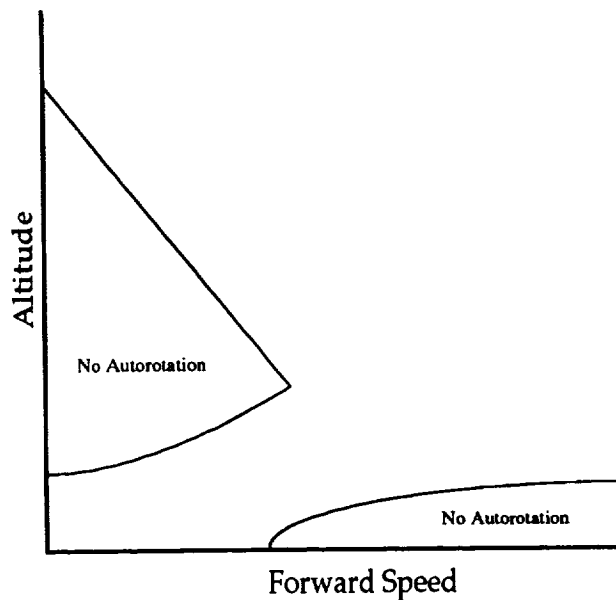


Figure 3.13: Deadman's Curve for a Typical Rotorcraft

A safe landing by autorotation is only possible if power is lost at certain combinations of altitude and forward speed. These combinations for a typical helicopter are shown in Figure 3.13. As seen in this figure, autorotation from all but very low altitudes requires forward speed. Therefore, in helicopters, flight is only authorized at altitude and forward speed combinations that allow for a safe, power-out landing.

The aerodynamic torque and corresponding thrust available from a rotor during autorotation are compromised by the high blade twist of conventional rotors. Helicopters, which are all required to autorotate, have a low twist compared to tiltrotors as seen in Figure 3.14.

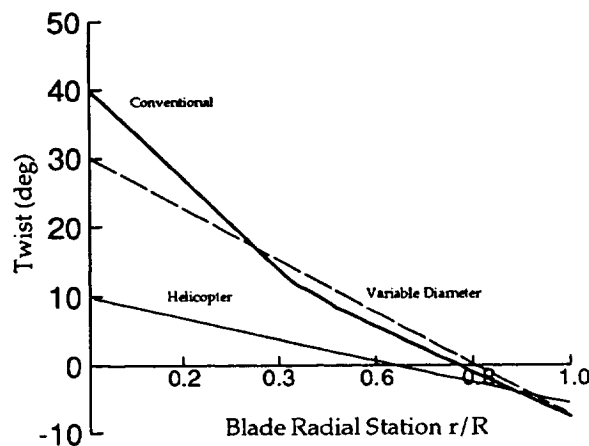


Figure 3.14: Blade Twist Comparisons

The effect of blade twist on rotor torque is seen by looking at the forces acting on different rotor sections during autorotation. Since the inflow angle varies with the rotational speed and twist along the rotor diameter, not all airfoil sections will experience the same forces. For this reason only the mid portion of the rotor actually

autorotates. As shown in Fig. 3.15, on the outer portion of the blade, the high rotational speeds result in a low inflow angle and only a small tilt of the lift vector.

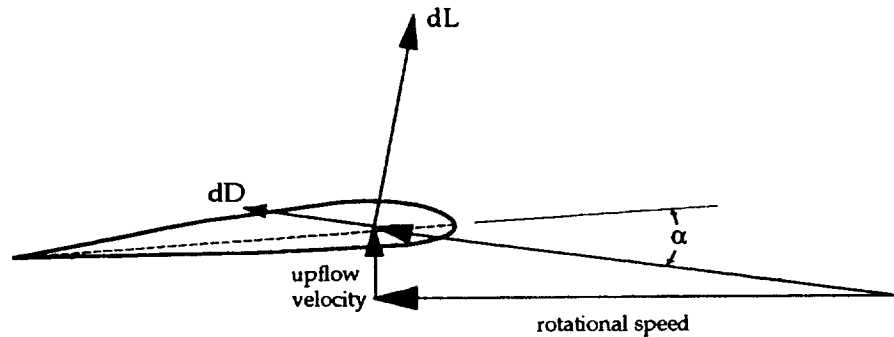


Figure 3.15: Forces During Autorotation in the Deceleration Region

Here the profile drag has a larger component in the rotor plane than the lift vector, and the resulting force tends to decelerate the rotor. On the inner portion of the rotor, the rotational velocity is low and the resulting angles of attack are above stall. As a result, these sections increase the drag on the rotor while contributing very little to the thrust. Due to the high twist of a conventional tiltrotor blade, the stalled region grows at the expense of the acceleration region. The conventional rotor not only produces less thrust for the same applied torque, but will also require a higher forward speed and rotor angle of attack to produce that torque. The variable-diameter rotor has a smaller stall region due to both a lower twist and a blade root cut-out. The approximate relative size of these regions for the two rotors are illustrated in Figure 3.16.

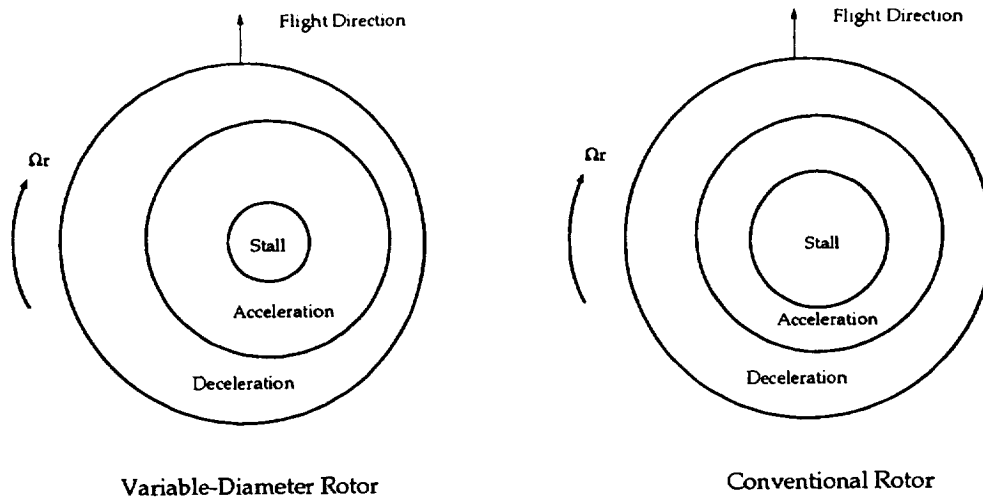


Figure 3.16: The Aerodynamic Regions of a Rotor During Autorotation

Using a sophisticated blade element analysis, the Sikorsky Aircraft Corporation calculated the thrust capability of an isolated conventional and variable-diameter rotor during an unpowered descent [29]. The conventional rotor model was based on published V-22 geometry, and the variable-diameter design was based on a rotor with a disk loading of 10 psf. The results are shown in Fig. 3.17 and Fig. 3.18 for a complete range of collective pitch. As expected, the larger stalled region of a conventional design has a significant effect on the available thrust during autorotation. In fact, the isolated conventional rotor could not produce enough thrust to balance the force of gravity and maintain a constant rate of descent from any flight condition. The variable-diameter design was found to be capable of supporting a larger percentage of the vehicle gross weight over a larger range of forward speed and rotor angle of attack.

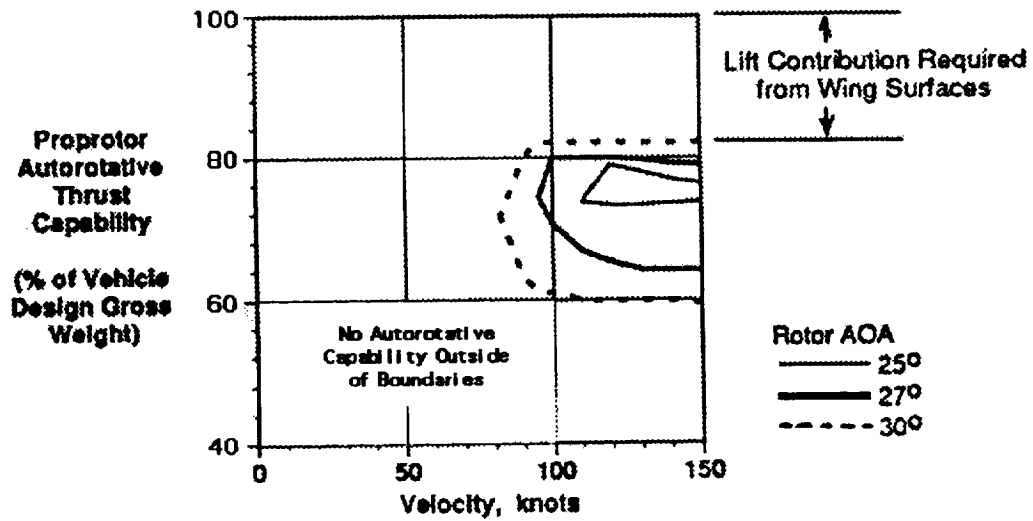


Figure 3.17: The Autorotative Thrust Boundary of a Typical Isolated Conventional Rotor

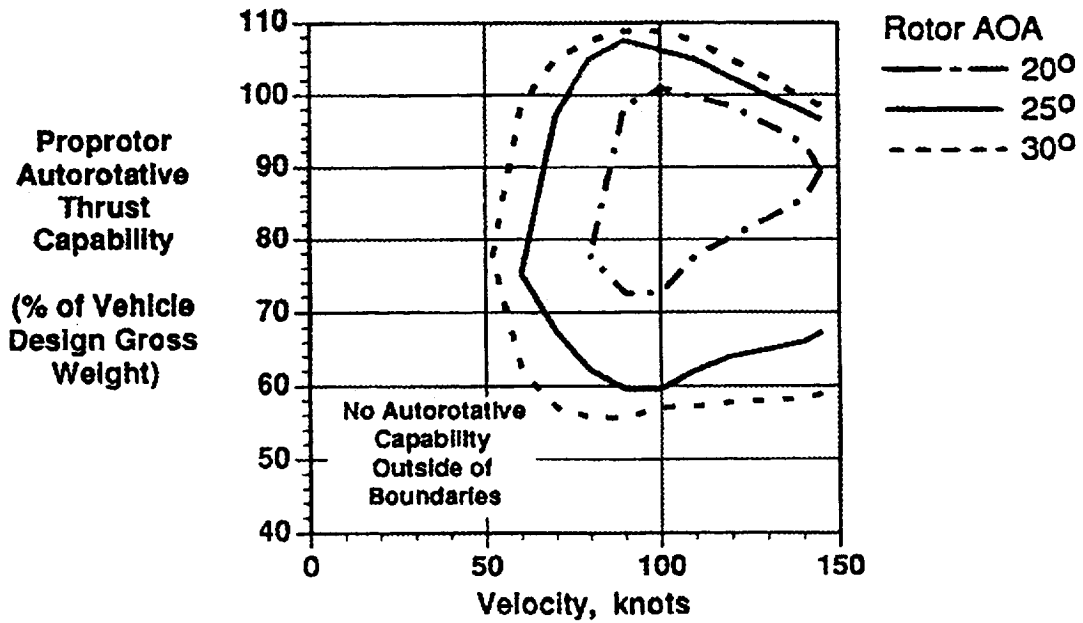


Figure 3.18: Autorotative Thrust Boundary of an Isolated Variable-Diameter Rotor

The analytical predictions of isolated conventional rotor thrust indicate that the airframe will have to provide some lift in order to support the total aircraft gross weight in autorotation. The results also show that the rotors will only have an autorotative thrust capability at high rotor angles of attack (20-30 deg). Assuming the nacelles could be tilted aft by 10 deg during descent, the airframe angle of attack would be 15-20 deg. At these high angles of attack, the airframe would likely be stalled which would limit the contribution it could make to supporting the weight of the aircraft in descent. If this is the case, it will be impossible to achieve a steady autorotative descent.

The rate of descent during a steady autorotative state is also critical to a safe landing. The rate of descent can be determined from the power required in autorotation which in turn depends on forward speed. The power required in an autorotative descent for a given forward speed is equivalent to the power required for forward flight at that speed. A typical power required curve for rotorcraft in forward flight is shown in Figure 3.19. In this figure the parasite power is the power required to overcome the drag of all non-lift producing components. Defined in terms of an equivalent flat plate area, f , the parasite power is

$$P_p = D_p V \quad (3.44)$$

where

$$D_p = f \cdot q = f \cdot \frac{\rho}{2} V^2 \quad (3.45)$$

As in hover, the profile power is the power required to overcome the viscous drag forces acting on the rotor blades. This power can be written as

$$P = D_o V \quad (3.46)$$

where D_o is the profile drag.

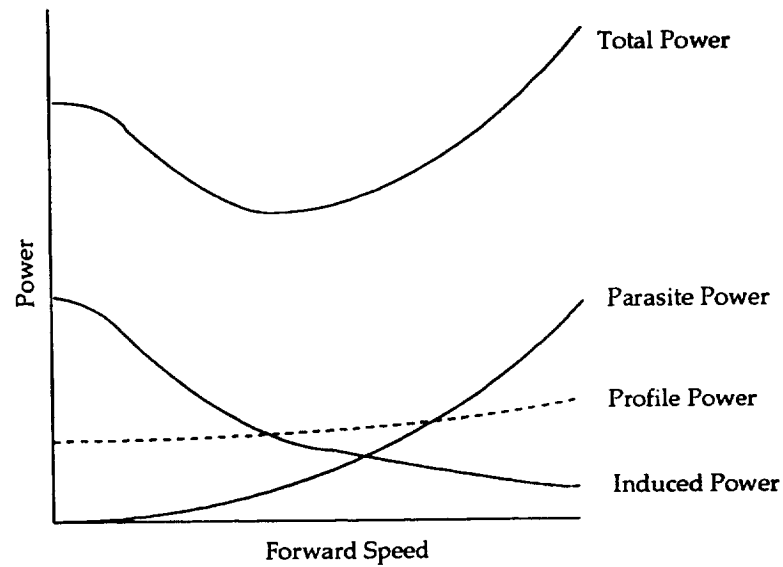


Figure 3.19: Power Required Curve for Helicopter Forward Flight

The induced power in forward flight can be estimated from momentum theory in a manner analogous to the method used for hover. Figure 3.20 shows the closed system considered in forward flight.

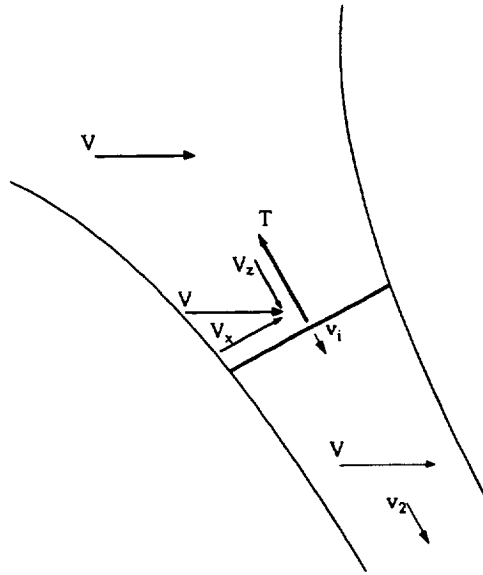


Figure 3.20: Momentum Theory Control Volume for Forward Flight

The induced thrust is equivalent to the mass flow multiplied by the velocity imparted to the airstream. To calculate the mass flow, the velocity through the rotor must first be determined. The velocity through the rotor is

$$V_R = \sqrt{V_x^2 + (V_z + v_i)^2} \quad (3.47)$$

or since $v_i \ll V$

$$V_R \cong V \quad (3.48)$$

Since the velocity imparted to the air is simply v_2 , the thrust becomes

$$T = \dot{m}v_2 = \rho AVv_2 \quad (3.49)$$

From the relationship between the induced velocity and v_2 given in Eq. 3.6, the thrust can also be written as

$$T = 2\rho AVv_i \quad (3.50)$$

The induced power is therefore

$$P_i = Tv_i = \frac{T^2}{2\rho AV} \quad (3.51)$$

Combining Eq. 3.44, Eq. 3.45 and Eq. 3.46, the power required for forward flight at a velocity, V , can be written as

$$P = \frac{T^2}{2\rho AV} + \frac{\rho}{2}fV^3 + D_oV \quad (3.52)$$

Since the power during autorotation is equivalent to the power required in forward flight, Eq. 3.52 also describes the power that must be supplied by the rotor in an engine out scenario. Therefore, the power for autorotation can be divided by the aircraft gross weight, W , to determine the rate of descent during autorotation:

$$\text{R.O.D.} = \frac{P}{W} = \frac{\text{D.L.}}{2\rho V} + f \frac{\rho}{2} \frac{V^3}{W} + \frac{D_o V}{W} \quad (3.53)$$

As seen in this equation, the forward speed corresponding to minimum power is desired in autorotation because it results in the minimum rate of descent. Furthermore, the rate of descent is shown to be directly proportional to disk loading which means for a similar profile and parasite power, the variable-diameter design will have a low rate of descent during autorotation.

The final, critical aspect of autorotation is the landing flare. The relative performance of an aircraft during a flare maneuver can be compared using a simple autorotative index. The index, developed by Fradenburgh [30], begins with an expression for the rate of descent based on momentum theory. The profile and parasite power are ignored. Since the forward speed, V , is optimized by the pilot, the rate of descent becomes a function of only disk loading and density:

$$\text{R.O.D.} = k_1 \sqrt{\frac{\text{D.L.}}{\rho}} \quad (3.54)$$

To eliminate the vertical descent velocity prior to landing, a vertical acceleration must be provided by the rotors over some time period Δt . This acceleration is given by

$$a_v = g \left(\frac{T - W}{W} \right) \quad (3.55)$$

where T is the rotor thrust provided and W is the aircraft gross weight. The acceleration multiplied by the time period over which it is applied must be equivalent to the change in velocity desired. Since the goal of the flare maneuver is to bring the rate of descent to near zero, the vertical acceleration provided must be

$$a_v = k_1 \sqrt{\frac{D.L.}{\rho}} \cdot \frac{1}{t_f} \quad (3.56)$$

where t_f is the duration of the flare maneuver. For a given maximum maneuver load factor that the aircraft can safely withstand, T/W , the flare time can be written as

$$t_f = \frac{k_2}{g} \sqrt{\frac{D.L.}{\rho}} \quad (3.57)$$

From Eq. 3.9 the power required to produce this load factor for a low forward speed, can be written as

$$P = k_3 W \sqrt{\frac{D.L.}{\rho}} \quad (3.58)$$

The energy required from the rotors is simply this power multiplied by the flare time, or

$$E_R = P \cdot t_f = \frac{k_4}{g} \frac{W \cdot D.L.}{\rho} \quad (3.59)$$

The source of this energy is the kinetic energy stored in the rotors. The energy available from the rotors can be written as

$$E_A = 2 \left(\frac{1}{2} I \Omega^2 \left[\left(\frac{\Omega_{start}}{\Omega} \right)^2 - \left(\frac{\Omega_{end}}{\Omega} \right)^2 \right] \right) \quad (3.60)$$

where I is the rotor polar moment of inertia of the rotor about the hub, Ω is the rotor speed during normal flight conditions and Ω_{start} and Ω_{end} are the rotor speed at the beginning and end of the flare maneuver. For a given percent rotor speed increase over normal at the beginning of the flare and decrease below normal at the end of the flare, the available energy can be rewritten as

$$E_A = k_5 I \Omega^2 \quad (3.61)$$

The amount that the energy available exceeds the energy required gives a good indication of the autorotative flare effectiveness of a helicopter.

$$A.I. = \frac{E_A}{E_R} = g\rho \frac{I\Omega^2}{W \cdot D.L.} \quad (3.62)$$

As seen in this equation, the energy ratio or autorotative flare index, A.I., improves with lower disk loading and higher rotor inertia. The variable-diameter design has a higher inertia rotor which increases the kinetic energy it absorbs for a given RPM increase during a landing flare. As discussed before, the lower disk loading also

reduces the rate of descent. This reduces the aircraft kinetic energy that must be absorbed by the rotors during the flare maneuver. During the final stage of the flare, when energy stored in the rotor is used to produce thrust, lower disk loading also lowers the hover power requirement. Therefore, the energy required to touch down without overloading the landing gear is significantly less.

3.5 External and Internal Noise

Several factors determine the noise produced by a rotor. Blade geometry and operating conditions such as advance ratio, flight path and nacelle tilt each have an effect. Unique characteristics of variable-diameter rotors such as low tip speed, low hover disk loading and the ability to adjust blade diameter during descent could lead to a reduction in noise levels over current conventional designs.

3.5.1 Harmonic Noise

Harmonic noise is one of the major noise sources in rotorcraft. The mechanisms that generate harmonic noise can be grouped into two principal categories: thickness noise and loading noise. Thickness noise is the result of a rotor blade changing the momentum of the surrounding fluid. The momentum imparted to the air is dependent on the blade geometry and motion. The loading noise is due to the time varying nature of the force distribution (lift and drag) acting on the blade. Thus, the loading noise and thickness noise are generally comprised of harmonics of the blade passing frequency. Both of these noise mechanisms depend on the rotor rotational speed.

Lowering the speed decreases the noise produced. Although these noise sources are important during hover, they do not produce highest tiltrotor noise levels.

3.5.2 Blade-Vortex Interaction

Flight tests of the XV-15 show that tiltrotor noise levels are highest during descent [31]. This is due to blade-vortex interactions (BVI) which occur as the rotors move through the tip vortices shed by other blades. BVI noise typically occurs only during descent, since in other flight modes the vortices are blown out of the rotor path. BVI noise is significant because it propagates for long distances ahead of the approaching aircraft at frequencies that humans find the most annoying.

One method shown to be effective at abating BVI noise is to alter the conversion flight profile. The highest noise levels of the XV-15 were found to correspond to nacelle angles of 60 degrees and high forward speeds. Simply decreasing the flight speed for all nacelle angles above 20 degrees resulted in a 30 percent decrease in the 75 dB Day-Night Average Sound Level noise footprint [31]. For civil tiltrotors operating in commercial and residential areas, the BVI noise will have to be reduced even further.

Other methods for reducing BVI noise have been suggested by Hardin and Lamkin [32]. One such method is to reduce the strength of the rotor tip vortices. Modification of the blade tip has shown some benefit for this approach [33]. A better method is to reduce the forces acting on the rotor at the time it encounters a vortex. This can be accomplished by increasing the number of blades or lowering the disk loading. Lowering the disk loading is the preferred method because increasing the number of blades would also increase the number of interactions. Although Hardin

and Lamkin realized it would be difficult to implement, they also noted that moving the trailing blade by a small distance so that it would miss the preceding vortex would be another effective means of decreasing BVI noise.

With a variable-diameter rotor all of these BVI reduction methods are possible. The rotor tip shape is not constrained because the torque tube spar stops well before the tip in the retracted position. A larger rotor diameter is maintained even at a 60 degree nacelle tilt angle (see Fig. 4.1) so the rotor will have a low disk loading when BVI is most likely. Finally, since the diameter of the individual blades can be varied, it is conceivable that changing the diameter of opposite blades could alter the blade vortex interaction region or cause the blade and vortex to miss one another completely.

3.5.3 Internal Noise

A primary contributor to the noise transmitted into the cabin is the amount of clearance between the fuselage and the rotor tips. The least amount of clearance will be during cruise when the nacelles are forward. For a wing span of 54 ft, a 53 ft variable-diameter rotor with a 66 percent retraction ratio could have a clearance of 5 ft as opposed to a clearance of only 2 ft for a 41 ft conventional rotor. Some of this clearance benefit would be offset by additional noise caused by the higher blade loading of the variable-diameter design. In either case, to achieve the recommended cabin noise level of only 78 dB [5], some type of acoustic treatment will be required. This would likely involve insulation, however, active noise suppression could also be used. The lowest near-field noise level possible is desirable because acoustic treatment just adds more weight to the aircraft.

Chapter 4

Aircraft Size and Performance Comparison Setup

The advantages of a variable-diameter rotor system have been discussed in detail. What remains unclear is the extent that added rotor system weight and complexity would offset potential benefits. To study the effects of additional rotor weight on overall system performance, a multidisciplinary conceptual aircraft design program was used to calculate the size and performance of variable-diameter tiltrotor aircraft.

Since reducing the disk loading of conventional tiltrotor designs may be another means of improving tiltrotor viability, conventional tiltrotor aircraft with a range of disk loadings were also sized in this study. The low disk loading conventional designs would enjoy many of the same advantages of the variable-diameter rotor in hover. However, they also have a penalty in cruise performance and, similar to the VDTR, they would add substantial weight to the aircraft. Very low disk loading designs may not be feasible because of aeroelastic stability problems with the long wings and rotors. Nevertheless, it is worthwhile to investigate the possibility to see what performance they could provide in the best case relative to a VDTR.

The following chapter discusses the setup for comparisons of the VDTR and conventional tiltrotor designs over a range disk loadings. To begin the conceptual design code used is discussed in detail. Next the implementation of the code for both the VDTR and conventional designs is presented.

4.1 VASCOMP

The conceptual design program used in this study is the NASA Ames version of the V/STOL Aircraft Sizing and Performance Computer Program (VASCOMP). This program was originally developed in 1968 by Boeing Vertol under a NASA contract to assess the feasibility of various V/STOL aircraft configurations [34]. Later, it was revised by Boeing in 1971, 1973 and 1980. The code is capable of analyzing a broad range of V/STOL aircraft including tiltrotors, tiltwings, and others using various combinations of turbojet, turbofan or turboshaft engines for lift and propulsion. Recently VASCOMP was modified at the NASA Ames Research Center. The most significant modifications included a conversion performance module, more thorough drag calculations, an improved wing weight module and a numerical optimizer.

4.1.1 VASCOMP Sizing

VASCOMP can be used to calculate aircraft size and performance for a given mission or to determine the mission capabilities of an aircraft with a predetermined size and performance. In this study VASCOMP's sizing capability is used.

The sizing process begins with a detailed set of aircraft inputs including quantities such as the number of passengers, horizontal and vertical tail volume coefficients, rotor efficiencies and an initial gross weight guess. Separate geometry, aerodynamics, propulsion, weights and mission modules are then used to synthesize an aircraft. First, the geometry module calculates aircraft dimensions according to user-defined wing, rotor, fuselage, and tail section dimensioning information. The user controls rotor dimensions by either specifying rotor diameter or hover disk

loading. Wing dimensions can be specified directly by inputting span and aspect ratio or indirectly by inputting a desired wing loading. Horizontal and vertical tail areas may be input directly or calculated from the following volume coefficients:

$$c_{VT} = \frac{L_{VT} S_{VT}}{B_w S_w} \quad (4.1)$$

$$c_{HT} = \frac{L_{HT} S_{HT}}{\bar{c}_w S_w} \quad (4.2)$$

In the above equations L_{VT} and L_{HT} are the moment arms from the aircraft center of gravity to the aerodynamic center of the vertical and horizontal tails, B is the wing span, \bar{c}_w is the mean wing chord and S_w , S_{VT} and S_{HT} are the unknown planform areas of the wing, vertical tail and horizontal tail respectively. Once the dimensions are set the aerodynamics module calculates the total aircraft drag coefficient and the engine sizing module chooses an engine size to meet hover, cruise or conversion power requirements. The weights module then estimates the empty weight of the aircraft by calculating individual component weights. A fuel weight available is then determined by the equation

$$W_{fuel} = W_{gross} - W_{empty} - W_{payload} - W_{useful\ load} \quad (4.3)$$

where the useful load includes the weight of the crew as well as passenger service items like water, beverages and food trays. Finally the performance module calculates the fuel weight required to perform each segment of the specified mission profile.

The sizing is considered to have converged on a feasible design if the fuel weight required is less than or equal to the fuel weight available. If not, a new gross weight estimate is made based on the discrepancy in the fuel. Fuel weight is the governing parameter for design convergence because the mission the aircraft must perform is predetermined by the user. Once the design has converged, the code prints out a detailed description of the aircraft geometry, weights and mission performance.

A numerical optimizer can be used in conjunction with the sizing routine to optimize any performance characteristic such as gross weight or direct operating costs before the design is considered to have converged. The optimizer is tolerant of highly non-linear objective functions with discontinuities in slope often found in VASCOMP [35]. The algorithm uses an unconstrained minimization technique with penalty functions. A variation of the conjugate gradient method and line searches are used to zero in on the objective function minimum. If the conjugate gradient method fails, the algorithm continues with direct pattern search.

4.1.2 VASCOMP Weight Estimation

In VASCOMP the weights of most aircraft components are calculated using statistical weight trend equations developed from data on existing aircraft and rotorcraft. For instance, rotor and hub weight are based on trend equations used in the Helicopter Sizing and Performance Program (HESCOMP) [36]. Rotor weight is a function of rotor radius, solidity and maximum thrust during maneuver while hub weight depends on the largest value rotor RPM squared times power. Drive system weight follows a trend based on required engine torque. Engine weight is assumed to be a linear function of engine horse power. The weight of fixed equipment such as air-

conditioning, seating and lavatories is also included. Fuselage weight is based on a diameter and length input by the user, a calculated cabin acoustic treatment weight required to maintain a desired internal noise level and a structural weight required to maintain a constant internal cabin pressure. Cabin acoustic treatment is a function of rotor diameter, tip speed, engine horse power and rotor-fuselage tip clearance. The weight of the tail section is a function of tail loads, pitch and yaw radius of gyration, dive speed and aircraft gross weight.

Trend equations are not practical for tiltrotor wing weight estimation. Too few of these aircraft exist to provide an adequate data base. Conventional aircraft wing weight trends are not useful since tiltrotor wing structure is likely to be determined by a torsional stiffness requirement for whirl flutter stability rather than a bending strength requirement. For a realistic wing weight estimate, VASCOMP incorporates a method developed by Chappell and Peyran which is based on the scaling of wing frequency ratios [37].

In the frequency ratio method the conceptual wing is treated as a cantilever beam with a tip mass representing the engine. A complex whirl flutter analysis is avoided by choosing beam bending and torsional stiffness to achieve desirable ratios between vibration frequencies and rotor speed. The method assumes that scaling conceptual wing frequencies such that

$$\left(\frac{f}{\Omega}\right)_{\text{conceptual}} = \left(\frac{f}{\Omega}\right)_{\text{reference}} \quad (4.4)$$

provides a reasonable assurance of aeroelastic stability. In the above equation, f represents a bending or torsion frequency and Ω is the rotor rotational speed. The

reference aircraft is an actual tiltrotor aircraft known to be stable. The frequencies of the first vertical, horizontal and torsional bending modes of a cantilever beam with tip mass are given by the respective equations

$$f_v = \sqrt{\frac{24(EI)_v}{L_w^3 m_t}} \quad (4.5)$$

$$f_h = \sqrt{\frac{24(EI)_h}{L_w^3 m_t}} \quad (4.6)$$

$$f_t = \sqrt{\frac{2GJ}{L_w m_t r_g^2}} \quad (4.7)$$

where L_w is the length of the beam (wing), m_t is the tip mass and r_g is the radius of gyration of the tip mass. Combining Eq. 4.4 with Eq. 4.5 - 4.7 yields the following ratios from which the required stiffness in torsion and the two bending directions of the conceptual wing can be determined:

$$\left[\frac{(EI)_v}{\Omega^2 L_w^3 m_t} \right]_{\text{conceptual}} = \left[\frac{(EI)_v}{\Omega^2 L_w^3 m_t} \right]_{\text{reference}} \quad (4.8)$$

$$\left[\frac{(EI)_h}{\Omega^2 L_w^3 m_t} \right]_{\text{conceptual}} = \left[\frac{(EI)_h}{\Omega^2 L_w^3 m_t} \right]_{\text{reference}} \quad (4.9)$$

$$\left[\frac{GJ}{\Omega^2 L_w m_t r_g^2} \right]_{\text{conceptual}} = \left[\frac{GJ}{\Omega^2 L_w m_t r_g^2} \right]_{\text{reference}} \quad (4.10)$$

Once the required stiffnesses are known, the corresponding area moments of inertia for a given material are easily determined. These moments of inertia are then related to torque box and spar cross-sectional areas by form factors based on tiltrotor wing airfoil data. Torque box and spar weights can be calculated from these cross-sectional areas. After sizing the torque box and spar to obtain the appropriate frequency ratios, the bending strength of the wing is checked for cruise and a 2g jump take-off. Here the maximum moment experienced is compared to the ultimate strain of the spar and torque box. Additional material is added if required.

This method of wing weight estimation works well if the conceptual aircraft is similar to the reference aircraft. Calculated wing weights for the XV-15 matches the true weight exactly and the V-22 estimate has less than a 0.1 percent error [37]. Estimates of conceptual aircraft wing weights will likely have more error, but as long as the configuration of these aircraft is similar to a reference aircraft, the errors should fall within the tolerance of a conceptual design.

4.1.3 VASCOMP Aerodynamics

Aircraft drag in cruise is calculated from the sum of induced, parasite and compressibility drag. The total drag coefficient can be written as

$$C_D = \frac{C_L^2}{AR \cdot \pi \cdot e} + \Delta C_{D_c} + C_{D_p} \quad (4.11)$$

where the first term is the induced drag, ΔC_{D_c} is the drag coefficient increase due to compressibility effects and C_{D_p} is the drag of the wing and all other airframe

components. The Oswald span efficiency factor, e , may be input by the user or calculated by the program. For tiltrotors it is best to input the Oswald number since these aircraft have a lower induced drag than predicted by conventional aircraft wing theory due to nacelle interference at the wing tips and interaction of the wing and rotor wake. As long as the rotors rotate so the blades move upwards in front of the wing, the swirl in the rotor wake will reduce the wing induced velocity [38]. The result is that the wing lift vector is tilted forward reducing the wing induced drag. The engine nacelles also reduces the induced drag because they interfere with the vortices shed at the wing tips. The parasite drag calculation for all components considers Reynolds number and 3-dimensional flow effects. Drag increases due to nacelle-wing, fuselage-wing and spinner-blade root interference are also accounted for. The compressibility drag coefficient is assumed to increase cubically as the cruise Mach number exceeds the drag divergence speed. The divergence speed is assumed to decrease linearly with the wing lift coefficient.

4.1.4 VASCOMP Propulsion

VASCOMP has several options for the calculation of rotor propulsive efficiency and figure of merit. The calculation can be based on actual propeller performance by using tables of rotor power coefficients as functions of thrust coefficient and advance ratio. Alternately, the user may specify point values for rotor efficiencies. These values include a figure of merit to be used in hover calculations, separate propulsive efficiencies to be used in climb and descent and a table of propulsive efficiencies versus flight Mach number to be used in cruise performance calculations. Several

analytical performance methods can also be used including blade element theory and the momentum theory presented in Section 3.3.

Engine performance is calculated using the corrected parameter method [34, 39]. The power (SHP), fuel flow (W_f), gas generator RPM (N_1) and power turbine RPM (N_{II}) for a given flight condition are defined as

$$\text{SHP} = \delta \sqrt{\theta} \cdot f_1 \left(M, \frac{T}{\theta} \right) \quad (4.12)$$

$$W_f = \delta \sqrt{\theta} \cdot f_2 \left(M, \frac{T}{\theta} \right) \quad (4.13)$$

$$N_1 = \sqrt{\theta} \cdot f_3 \left(M, \frac{T}{\theta} \right) \quad (4.14)$$

$$N_{II} = \sqrt{\theta} \cdot f_4 \left(M, \frac{T}{\theta} \right) \quad (4.15)$$

where δ and θ are the density and temperature ratios between the given and a reference flight condition. The functions f_1 , f_2 , f_3 , and f_4 describe the engine performance at the reference flight condition for combinations of Mach number and turbine inlet temperature, T . Variations in engine power due to Reynolds number effects are accounted for by applying an appropriate correction factor to the shaft horse power. The engine “deck” in VASCOMP consists of tables of engine referred SHP, W_f , N_1 and N_{II} in tabular format. These referred values are just the functions f_1 , f_2 , f_3 and f_4 normalized by the engine maximum static sea level values of shaft horse power, fuel flow, gas generator speed and power turbine speed respectively. For a given flight

condition (Mach number) and an engine power setting (turbine inlet temperature), engine performance is calculated by a table look up followed by multiplication by the appropriate density or temperature ratio. Limits on gas generator speed, turbine speed, fuel flow and engine torque as well as engine contingency power may be specified by the user.

4.1.5 VASCOMP Conversion and Download

As pointed out in Section 3.2.3, interactions between the rotors, wings and fuselage have a significant impact on tiltrotor performance during hover and conversion. In VASCOMP these interactions are calculated in the conversion module in order to predict download and conversion performance.

The download calculation assumes the wake is fully contracted when it reaches the wing. At the wing the rotor wake is assumed to be turned toward the fuselage without any loss of momentum. At the fuselage the flow is assumed to be blocked and dispersed equally in all 180 degrees above the wing. The total momentum of the dispersed flow is then integrated to determine the download contribution. Increases in induced power caused by the fountain effect are assumed to be balanced by the partial ground effect provided by the wings.

Conversion performance is calculated at incremental velocity steps. The required nacelle tilt (thrust vector) at each velocity increment is calculated from a force balance on the aircraft. The force balance includes the lift and drag produced by the nacelles and wings at an angle of attack that takes into account rotor swirl. Download caused by the wake is calculated taking into account the effects of the wake falling off of the wing due to aircraft forward speed. The user specifies the acceleration profile to be

followed during the conversion. VASCOMP determines the conversion speed by first calculating the stall speed and then multiplying the stall speed by a user input margin of safety.

4.2 Comparison Approach

The variable-diameter and conventional tiltrotors compared in this study are derivatives of a NASA Short Haul Civil Tiltrotor (SH(CT)) baseline. The SH(CT) baseline mission, shown in Fig. 1.6 was assumed for all aircraft. The SH(CT) fuselage dimensions, cabin layout, high wing and t-tail were also common for all designs. The same level of engine performance was assumed although engine size was allowed to vary. The size and weight of the rotors, wings and tail were allowed to change with disk loading.

Although external noise was not calculated directly, the external noise issue was not ignored. Accurate noise predictions require details of the rotor geometry and loading that were not available at this early design stage. Wells, Bona and Glinka have developed a methodology that may be useful in predicting rotor acoustics for conceptual designs [40], however, the code is not yet fully integrated into VASCOMP and it is not set up to model variable-diameter rotors. Therefore, the accuracy of any quantitative noise predictions in this study would be highly questionable. In order to give proper treatment to the importance of external noise without calculating the noise directly, rotor characteristics and flight patterns known to lower noise were selected. Only Four-bladed rotors with low tip speeds relative to the V-22 and SH(CT) baseline were considered. As discussed previously, increasing the number of blades and lowering tip speed are methods of reducing BVI noise during descent and loading

noise during hover. Also, fairly steep 6 degree approach and departure paths were selected to lower community noise exposure. These design choices should result in acceptable noise levels for each of the low disk loading designs considered.

4.2.1 Common VASCOMP Inputs

A common engine model was used for both aircraft designs. The model was a generic turboshaft engine with a power rating appropriate for civil use. This engine deck was also used in the (SH(CT)) VASCOMP model. Engine size was “rubberized” to meet the largest power requirement of hover, conversion or cruise within set limits on engine power turbine speed, gas generator speed, inlet temperature and fuel flow. Power output was assumed to have a quadratic drop off as turbine speeds varied from the optimum. Therefore, lowering turbine speed during cruise to increase propulsive efficiency resulted in reduced engine efficiency. A 3.5 percent contingency power was assumed where contingency power is defined as

$$C.P. = \frac{2.5 \text{ min. power rating @ } 2000 \text{ ft ISA} + 20^\circ}{5.0 \text{ min. power rating @ } 2000 \text{ ft ISA} + 20^\circ} \quad (4.16)$$

A power to weight ratio and specific fuel consumption were assumed based on a year 2005 entry into service date.

Conversion between vertical and forward flight was found in a previous study to have a significant impact on tiltrotor sizing [9]. Although many important problems of conversion such as blade loads and stability are outside the scope of a conceptual design, conversion does generally require the most engine torque and therefore it sizes

the transmission. If an aggressive acceleration profile is followed, conversion power may even set the engine size. For both designs, conversion was allowed to size the engine and transmission if necessary. However, to avoid conversion engine sizing, a conservative conversion acceleration profile shown in Fig. 4.1 was used for both designs.

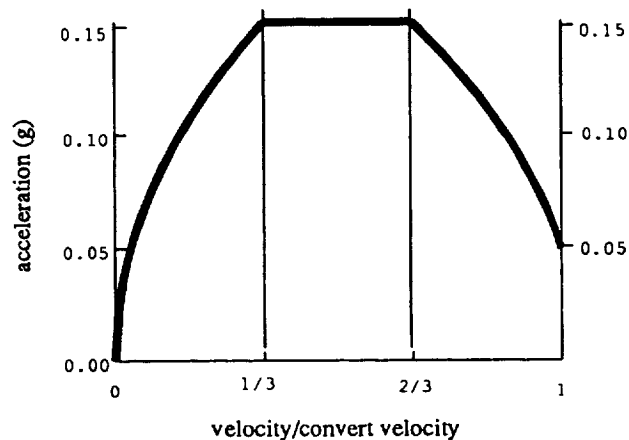


Figure 4.1: VASCOMP Conversion Acceleration Profile

For both types of aircraft, a cabin acoustic treatment weight was included in the gross weight calculation. The method used in VASCOMP for calculating the cabin treatment weight overestimates the weight predictions presented by Unger and Alexander for a 78 dB interior noise level [5]. The later calculations are assumed to be based on a more thorough analysis, so the VASCOMP calculation was adjusted. A better match was obtained by setting the target cabin noise level to 90 dB in the VASCOMP routine. The adjusted VASCOMP calculations agreed closely with those predicted by Unger and Alexander [5] for similar tip clearances and tip speeds. At

lower tip speeds or greater tip clearances any errors in the artificial estimate are carried through to both aircraft designs.

The V-22 was selected as the reference aircraft from which to scale the frequency ratios for whirl flutter wing sizing. To improve the accuracy of the weight calculation, the 23 percent wing thickness to chord ratio of the V-22 was assumed for all designs. A secondary reason was so the known compressibility drag characteristics of the V-22 wing could be used in the conceptual design. A high Oswald efficiency factor of 0.98 was assumed for all wing designs to account for the beneficial effects of the rotor wake swirl and nacelles on induced drag.

4.2.2 The Variable-Diameter Tiltrotor VASCOMP Model

Several VASCOMP calculations had to be modified to properly model VDTR aircraft. Variable-diameter rotor weights were calculated by simply applying a scaling factor to the VASCOMP rotor weight trend equations. As the increased rotor system weight was carried through the sizing modules, VASCOMP automatically made appropriate changes to other component weights. A scaling factor of 1.2 was selected for rotor and hub weight calculations based on estimates by Fradenburgh and Matuska [11]. They estimated variable-diameter rotors would weight 20 percent more than conventional rotors with the same radius, solidity and hover tip speed. This factor actually leads to a dramatic increase in rotor weight for the same airframe. For example, for a 54 ft wing span, a 53 ft variable-diameter rotor system weighed 3132 lb per rotor. For the same span, the 41 ft conventional rotor only weighted 2144 lb each. Therefore, the variable-diameter system resulted in a 46 percent increase in rotor system weight.

Rotor performance was calculated from point values of figure of merit and propulsive efficiency during climb, descent and cruise. The specific values of figure of merit and propulsive efficiency for a given C_T/σ were based on analytical predictions from an EHPIC/HERO analysis as described in reference [21]. The efficiencies and thrust coefficient assumed in this study are similar to those calculated for a rotor configuration also presented in this reference. The rotor design was assumed to have a 66 percent retraction ratio and a tip speed of 600 fps.

To model the variable-diameter-rotor diameter change during conversion, the VASCOMP conversion module had to be modified. The original module assumed a constant rotor diameter throughout the conversion sequence. Therefore, the rotor thrust and the inflow to the wing due the rotor wake were in error. To correct the problem, a nacelle tilt change schedule had to be input into VASCOMP. The schedule used is shown in Figure 4.2.

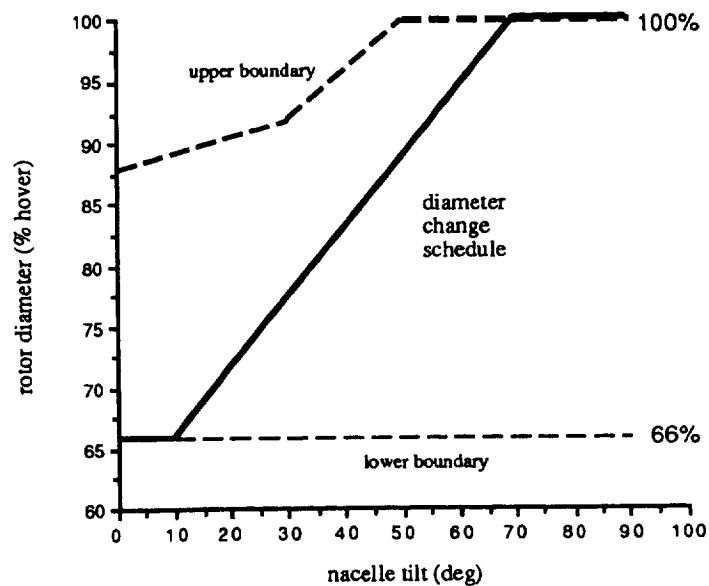


Figure 4.2: Diameter vs. Nacelle Tilt Schedule

There was no easy way to input this information into VASCOMP because the nacelle angle is not an independent variable in the conversion module. Rather, the module determines the required nacelle angle at a given velocity based on a force balance calculation. To avoid changing the method used in the module, a table of “best guess” nacelle tilt angle versus velocity was included in the VASCOMP input. This schedule could then be used to determine rotor diameter based on airspeed rather than nacelle tilt. After a program run was complete, the assumed profile was checked against the actual nacelle tilt schedule calculated by the force balance. If differences in the assumed tilt and calculated tilt were significant, the table was modified and the run was repeated. This procedure was easy to implement and worked fairly well since the calculated nacelle tilt versus velocity profile did not vary significantly for different variable-diameter designs. Samples of the conversion nacelle tilt schedule calculated by VASCOMP for variable-diameter and conventional designs are shown in Figure 4.3.

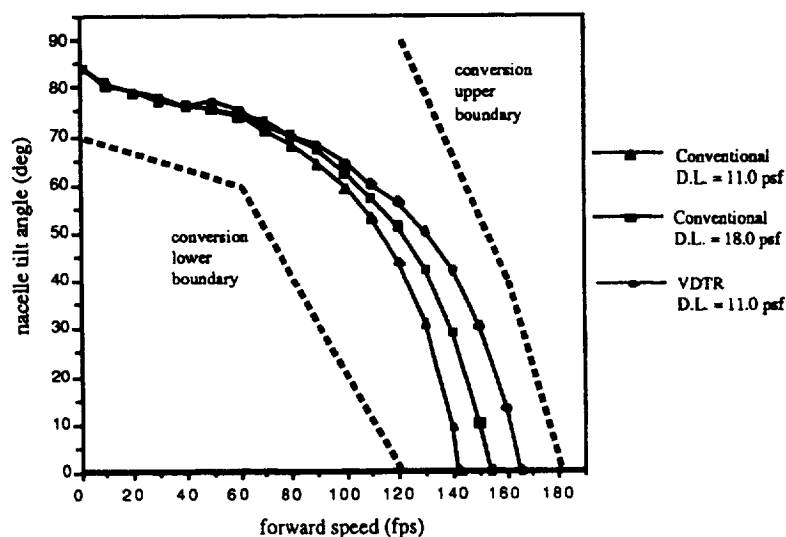


Figure 4.3: Nacelle Tilt vs. Forward Speed

The numerical optimizer was used in the variable-diameter designs to minimize aircraft gross weight with respect to wing loading and rotor tip clearance in hover. These design variables were selected to keep the wing aspect ratio at the optimum value. When disk loading was varied, wing span had to change with the rotor diameter. Allowing the tip clearance and wing loading to vary allowed VASCOMP to select the optimal corresponding wing span and chord. If these variables were held constant, the aspect ratio would be either too small, resulting in unnecessary induced and profile drag, or too large resulting in unnecessary wing weight. Hover tip speed was held at 600 fps because the optimal tip speed was always found to be higher than desirable for noise considerations. The remaining parameters were also held constant to keep the basic airframe of the SH(CT) baseline.

4.2.3 Conventional Tiltrotor VASCOMP Model

Conventional rotor performance was calculated using a Boeing Vertol rotor model included in VASCOMP. The model assumes V-22-like performance. In this method figure of merit is determined from a table of measured V-22 values over a range of blade operating thrust coefficient to solidity ratios and blade tip Mach numbers. The momentum theory discussed in Section 3.3 is used to predict propulsive efficiency for a given cruise flight condition. The calculation proceeds as follows. First the rotor profile torque coefficient is calculated from an input average blade profile drag coefficient and a rotor drag divergence Mach number. These two quantities completely define the profile torque (C_{Q_0}) for a given advance ratio and solidity. Since the torque coefficient (C_Q) is defined by engine capabilities, C_T can be

calculated directly from Eq. 3.42. Finally, with C_T , C_Q and μ defined, propulsive efficiency is calculated from Equation 3.34.

The numerical optimizer was also used on the conventional models to minimize aircraft gross weight. For the conventional design, hover tip speed and wing loading were allowed to vary. Tip clearance did not need to vary because the optimal value was always the minimum acceptable clearance of 2.0 ft. The wing loading of the conventional designs was allowed to vary for the same reasons as in the VDTR case. The choice of tip speed involves a trade off between drive system weight and wing weight. A low tip speed increases the torque requirement which drives up the drive system weight. A high tip speed increases the wing stiffness and weight required for whirl flutter stability. Tip speed was allowed to vary so that the weight of the high disk loading designs would not be penalized unfairly. As the results show, however, the optimal tip speed was relatively constant over the range of disk loading anyway.

Chapter 5

VASCOMP Results

In this chapter tiltrotor aircraft with conventional and variable-diameter rotors are compared based on VASCOMP sizing and performance predictions. Calculated weights and dimensions are first discussed for baseline aircraft. The autorotation index of both baselines is calculated to give a rough comparison of autorotative performance. Later, size trends for VDTR and conventional aircraft are presented over a range of hover disk loading values.

5.1 Baseline Aircraft Comparisons

To begin, baseline aircraft with conventional and variable-diameter rotors are compared. A summary of the aircraft considered is given in Table 5.1. The conventional aircraft described was selected as the conventional baseline because the wing, rotor, tail and fuselage dimensions were essentially the same as the NASA SH(CT). The only major differences in this design are the higher gross weight and disk loading which are primarily a result of using four-bladed rather than three-

bladed rotors. The VDTR baseline considered here is just the conventional baseline airframe equipped with variable-diameter rotors. The additional weight of the rotor system increased the optimal wing aspect ratio and decreases the tail size slightly, but other airframe dimensions remained the same.

	Conventional Baseline	VDTR Baseline
Hover Disk Loading	18.0 psf	11.0 psf
Wing Loading	123 psf	133 psf
Hover Tip Speed	601 fps	600 fps
Fuselage Length	61.7 ft	61.7 ft
Horizontal Tail Area	426 sqft	455 sqft
Vertical Tail Area	441 sqft	458 sqft
Wing Span	54.4 ft	54.2 ft
Aspect Ratio	7.51	7.96
Hover Rotor Diameter	41.4 ft	53.2 ft
Cruise Rotor Diameter	41.4 ft	35.1 ft
Rotor Solidity	0.165	0.104
Download Ratio (D/W)	0.107	0.076
Hover Power Loading	0.424 lb/hp	0.327 lb/hp
Gross Weight	48334 lb	48883 lb

Table 5.1: Baseline Conventional and Variable Diameter Design Summary

VASCOMP results show that although the baseline VDTR and conventional designs are similar in dimension, they are very different in weight and performance. A detailed description of the weights of each design is given in Fig. 5.1 and Figure 5.2.

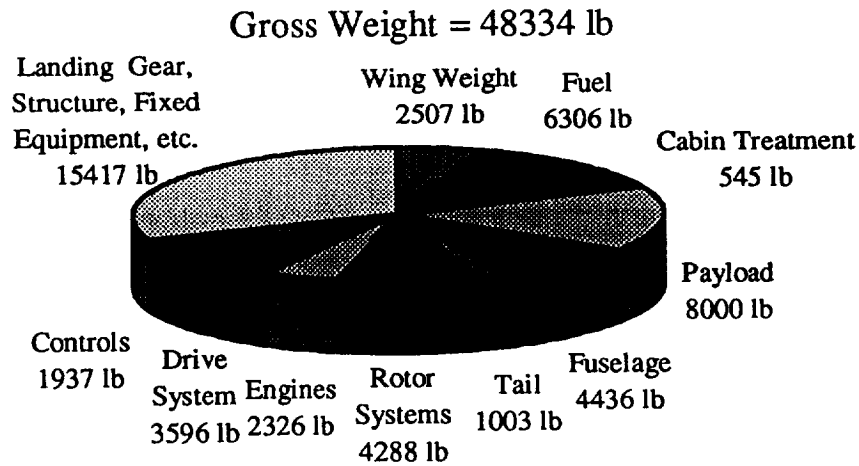


Figure 5.1: Conventional Rotor Baseline Aircraft Weights

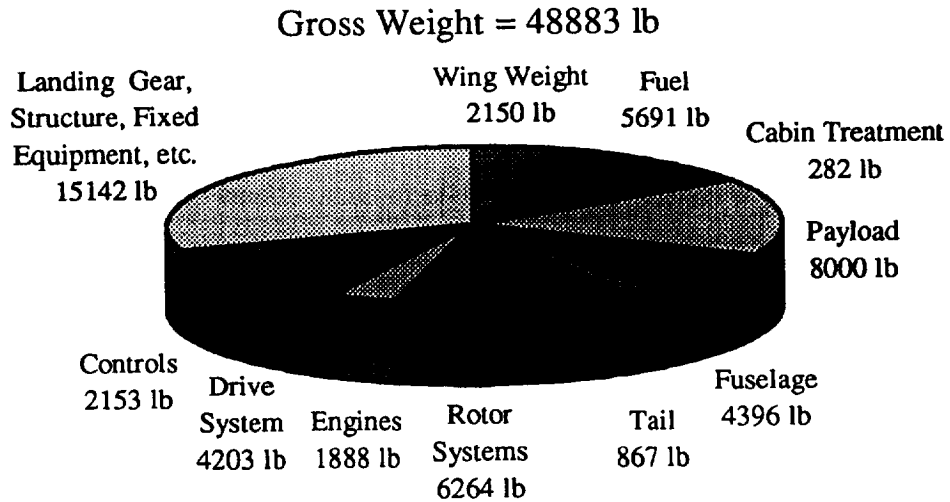


Figure 5.2: Variable-Diameter Rotor Baseline Aircraft Weights

The gross weight of the VDTR is slightly higher due to a 46 percent increase in rotor weight. The drive system weight is also 17 percent higher due to a higher torque

requirement during conversion as the diameter is reduced. However, much of the rotor and drive system weight penalty is offset by other factors. The wing weight is decreased by 14 percent because less wing stiffness is required for whirl flutter stability. The cabin acoustic treatment weight is reduced by 48 percent because of a larger fuselage-rotor tip clearance and reduced tip speed during cruise. The engine size is reduced because of a 22 percent decrease in the hover power requirement. The drop in power is due to a decrease in induced power and download to thrust ratio. A smaller engine combined with a higher rotor propulsive efficiency also decreases the fuel requirement of the VDTR. The 9.8 percent decrease in required fuel relates directly to a decrease in operating cost. The VDTR has a lateral shaft spacing of 2.04 rotor radii and should experience as much as a 20 percent decrease in power at advance ratios between 0.03 and 0.16. The conventional baseline will not experience this reduction in induced power because the lateral shaft spacing is 2.63 rotor radii. With the beneficial interference effects of the side by side rotors accounted for, the power difference between the baseline designs in this advance ratio range could be as much as 33 percent. This means the VDTR is a good way to meet OEI flight requirements without the need for high levels of contingency power.

During recent simulations of the VDTR in the Vertical Motion Simulator (VMS) at the NASA Ames Research Center, it was found that the maximum power required through the transmission during conversion was similar to the hover value. This is in conflict with VASCOMP results which indicate conversion requires 910 more hp through each transmission. Although hover sizes the engines due to the

OEI power requirement, the higher power through the transmissions leads directly to an increase in the VASCOMP calculated drive system weight. If the VMS mathematical model is assumed to represent conversion more accurately, the calculated VDTR baseline drive system weight is incorrect. To determine the impact a lower conversion power requirement would have on the VDTR baseline, the VASCOMP conversion drive system sizing option was disabled and the VDTR baseline size was recalculated. The resulting design had a gross weight of 47,090 lb, a 3.7 percent reduction from the VDTR baseline value. The conventional baseline gross weight was unaffected by this change since its drive system was already sized by hover. Therefore, if the actual VDTR conversion power is near the hover value, a variable-diameter rotor system will lead to a 2.6 percent reduction in gross weight for the conventional baseline design rather than a 1 percent increase as indicated previously.

Another important basis for comparison of the baseline aircraft is their performance in autorotation. As discussed in Section 3.4, autorotation involves three distinct phases. These are the pilot reaction period immediately after engine failure, the steady autorotative descent and the flare maneuver. Performance in the first and last phases is heavily dependent on the energy that can be stored in the rotor. The second phase depends on the autorotative thrust capability of the rotor, the contribution from the wing and the aircraft parasite drag.

The rate of descent is not calculated here because it would require a detailed trim analysis which is beyond the scope of this study. However, it has already been

shown that the isolated variable-diameter rotor could generate more thrust during an autorotative descent than a conventional V-22 size rotor (see Fig. 3.18-3.19). This is a good indication that the VDTR will have a much lower rate of descent at a given forward speed than a conventional rotor.

The effectiveness of a flare maneuver and the time a pilot has to react to a power failure are heavily influenced by the rotor mass moment of inertia. The rotor moment inertia was determined from the VASCOMP calculated rotor weights assuming that the mass of the rotor blades was evenly distributed along their length. This assumption is probably good for the VDTR rotor, but it may overestimate the conventional rotor inertia because more of the mass should be found inboard. For the VDTR baseline aircraft, the weight of a single blade was 397 lb which corresponds to a mass moment of inertia of 11,620 slug-ft² per rotor. For the conventional baseline, the weight and inertia were 259 lb and 4596 slug-ft² respectively.

Pilot reaction time depends on the amount of kinetic energy stored in the rotor and the rate of kinetic energy decay due to losses at the blades. Assuming the rate of energy loss is similar for both aircraft, the pilot would have more than twice the time to react in the VDTR baseline.

Along with the rate of descent, the rotor inertia plays a major role in the landing flare maneuver. The Autorotative Flare Index is easily calculated for both designs using Eq. 3.62 [30]. The acceleration due to gravity and the density are omitted assuming that the flare maneuver takes place at sea level. Based on the

gross weight, disk loading and rotor speeds indicated in Table 5.1, the Autorotative index for the VDTR baseline is 21 ft³/lb while it is only 9.50 ft³/lb for the conventional baseline. The VDTR index is comparable to the index for a large helicopter such as the Sikorsky CH-53D at a slightly lower gross weight. The conventional baseline index is far below the range of even the heaviest helicopters. The conclusion of this energy based analysis is that a conventional rotor would have a questionable ability to arrest an autorotative descent while the VDTR will likely have the autorotative performance of a heavy helicopter.

5.2 Comparison Over a Range of Hover Disk Loading

As discussed in the preceding section, the increased rotor weight of the VDTR leads to a small (less than 1 percent) increase in gross weight over the baseline aircraft. In contrast, this section shows that if a low disk loading is forced on a conventional design the VDTR compares favorably in terms of gross weight. This is because a conventional design incurs a significant wing weight penalty as disk loading is reduced.

In the following comparisons it is important to consider the error inherent in a conceptual design code such as VASCOMP. Errors could be introduced in several calculations. For instance, although the analytical method used to compute conventional rotor propulsive efficiency correlates well with empirical data from the V-22, the agreement with much larger rotors can be expected to be less exact. Other

possible sources of error are the engine performance and figure of merit which are found by fitting a quadratic curve to tabular data. Errors inherent in the curve fit were found to over estimate the figure of merit by as much as 0.02. Perhaps the largest source of error is in the estimation of component weights based on trend equations. While most aircraft components follow a definite trend, aircraft outside the range of experience may not fit these trends. For the range of disk loading considered here, the conventional rotor diameter range is outside the range of V-22 experience: the rotor diameters range from 6 percent to 69 percent larger than the 39 ft diameter V-22 rotor. In the V-22, oscillatory rotor loads can exceed the rotor load limit during aggressive maneuvers. To prevent failure, pilot inputs during maneuvers must be limited by an automatic control system [41]. This situation should be much worse as the cruise rotor diameter increases. Without a proper static and dynamic loads analysis, wing, rotor and hub weights may be inaccurate. For the VDTR, dynamically-scaled-model wind tunnel tests have at least demonstrated stability and acceptable blade loads for the size of rotors considered here [19]. In addition, except for the lowest disk loading case, all of the variable-diameter rotors considered are actually smaller than the V-22 rotor in the cruise configuration. This increases confidence that blade loads will be acceptable. The large diameter hover rotor of the VDTR is not as much of a concern because it is in the range of helicopter experience. Another possible error is the wing weight calculation. As discussed in the following paragraphs, the wing of the conventional design was always sized by whirl flutter while the VDTR wing was always sized by bending.

The calculated VDTR wing weight should be more accurate because it is easy to predict wing response to a static load. It is much more difficult to predict the input force and the wing response resulting from the gyroscopic motion of the rotor pylon as in whirl flutter.

There are also possible errors in the VDTR calculations. As mentioned before, the VDTR rotor weight was calculated by simply applying a 20 percent penalty to what the weight would have been if the diameter did not change. In reality this penalty could vary significantly depending on the diameter change mechanism. The VDTR may also have a slightly different download than calculated by the VASCOMP model due to a reduction in the fountain. In the absence of experimental data, possible losses in rotor thrust caused by the fountain were ignored.

Although it is difficult to estimate the size of the possible errors, it will be assumed that the relative size and performance calculations are only accurate to within +/- 1 percent. For the designs considered here, the comparison error is in the range of 480-540 lb. Of course the absolute magnitudes of the weight calculations are probably much higher. The VASCOMP calculated aircraft size is likely to be only within 5 to 10 percent of an actual aircraft.

A summary of the VDTR and conventional tiltrotor designs considered is shown in Table 5.2. The fuselage diameter and length were held constant for both designs. The wing loading was optimized in both cases while the tip speed was optimized only for the conventional design. The fact that the tip speed of the VDTR

was fixed had a negligible effect on the results. If the conventional design tip speed were also fixed at 600 fps the maximum gross weight increase for any design would have been less than 0.23 percent.

	Disk Load (psf)	Wing Load (psf)	Tip Speed (fps)	Wing Span (ft)	Aspect Ratio	Diameter (ft)
Conventional						
	18.0	122.5	601	54.4	7.51	41.4
	16.0	110.5	613	56.8	7.42	43.7
	14.0	98.1	632	59.8	7.31	46.7
	12.0	97.0	612	63.7	8.15	50.6
	11.0	98.0	602	66.3	8.80	53.2
	10.0	97.5	599	69.6	9.41	56.5
	8.0	89.7	596	78.7	10.27	65.6
Variable Diameter						
	14.0	148.8	600	49.2	7.35	47.2
	12.0	135.0	600	52.8	7.71	50.1
	11.0	132.5	600	54.2	7.96	53.2
	10.0	124.2	600	57.0	8.19	56.0
	8.0	106.0	600	65.0	8.71	63.9

Table 5.2: Conceptual Design Dimension Information

The gross weights of the designs are shown in Fig. 5.3. Within the error discussed, both designs are seen to have a relatively constant (+/- 500 lb) gross weight over a range of disk loading. For the conventional rotor, this range is from 12-18 psf. For the VDTR the range is from 10-14 psf. A surprising result is that the weight penalties of the conventional designs are less than the weight penalties of the

VDTR until disk loading is reduced to about 11 psf. As the disk loading is reduced to 8 psf, the gross weight of both designs shows a dramatic increase. While it is acknowledged that this is certainly the likely trend, these designs have wing spans and rotor diameters so far out of the range of tiltrotor experience that there is little confidence in the gross weight estimate.

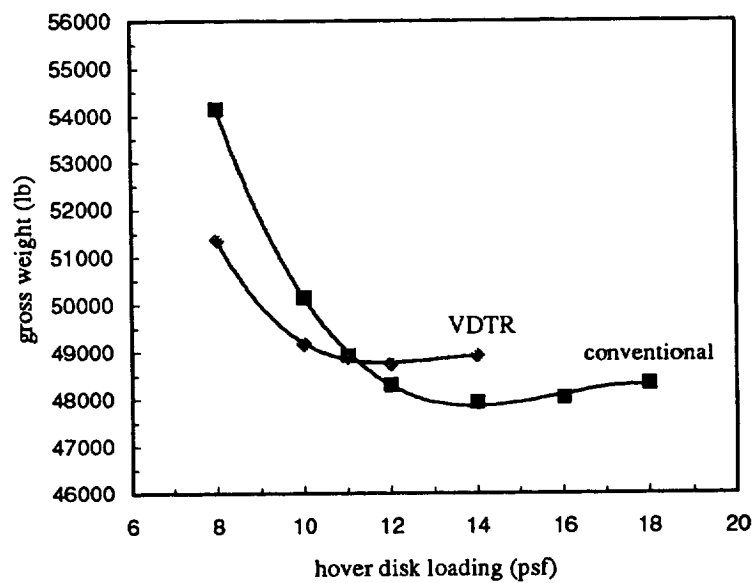


Figure 5.3: VASCOMP Calculated Gross Weight vs. Disk Loading

The trends for gross weight shown above can be explained by considering the wing weight trend seen in Fig. 5.4. The key is that the difference in the wing weight between the conventional and variable-diameter designs diverges with an increase in disk loading.

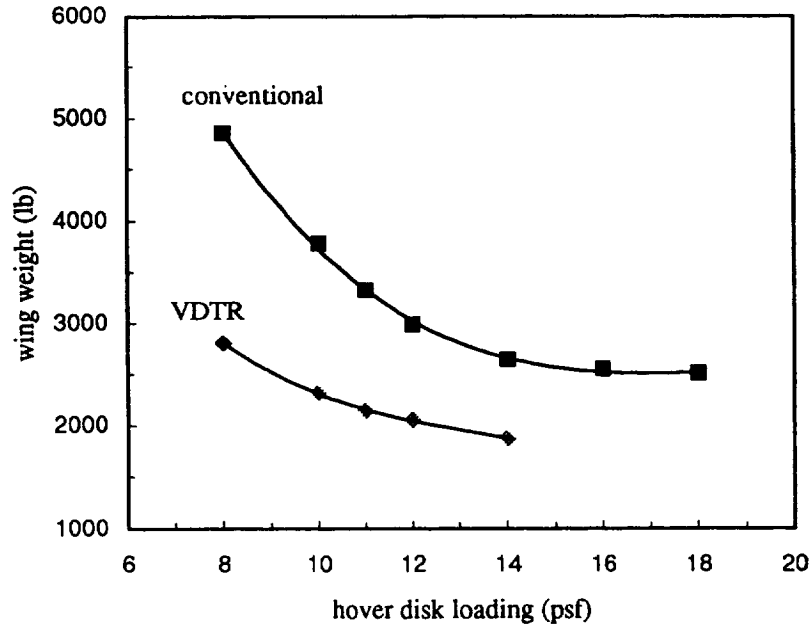


Figure 5.4: VASCOMP Calculated Wing Weight

The difference in the conventional and VDTR wing weights can be explained as follows. At a disk loading of 14.0 psf, the conventional wing span is slightly larger than the VDTR wing due to a larger cruise rotor diameter. In addition, the wing must be stiffer to guard against whirl flutter. As disk loading is reduced in the conventional design, increasing rotor diameter forces the wing span to increase which leads to a larger wing area and an increased profile drag during cruise. In addition, the rotor propulsive efficiency decreases because of a lower blade loading. The additional drag and reduced efficiency combine to increase the cruise power requirement. Near 11 psf the cruise power becomes so large that it exceeds the

hover power requirement. To minimize gross weight it becomes necessary to reduce the wing drag. This is done by increasing the wing aspect ratio (span/chord). Trends for the optimal aspect ratio and resulting wing drag are shown in Figure 5.5. The penalty of a higher aspect ratio is an increase in wing weight since it is more difficult to stiffen a long slender wing. In contrast, the VDTR engine is sized by hover at all disk loading values, and decreasing wing drag by increasing the wing aspect ratio has little benefit in terms of gross weight. The end result is that the wing weight increases faster for the conventional design as disk loading is reduced.

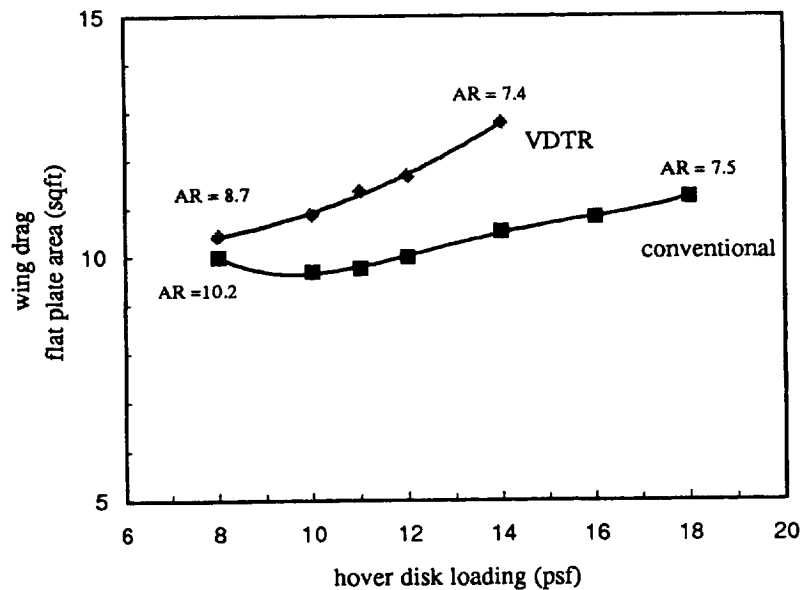


Figure 5.5: VASCOMP Calculated Wing Drag

If the wing loading would have been held constant as the disk loading was reduced, the weight penalty would have simply shifted to the engine and fuel weights due to a high cruise power requirement.

As discussed in Chapter 3, lower disk loading should reduce fuel, engine and acoustic treatment weight. This trend is verified in Fig. 5.6-5.8. The engine and fuel weight savings combined with the cabin acoustic treatment weight reduction tend to balance the wing and rotor weight penalties involved. This keeps the aircraft gross weight relatively constant over a range of disk loadings. However, once the hover disk loading is lowered to the point where the cruise power requirement exceeds the hover power, fuel and engine weight savings disappear. Lower disk loading only acts to worsen cruise performance.

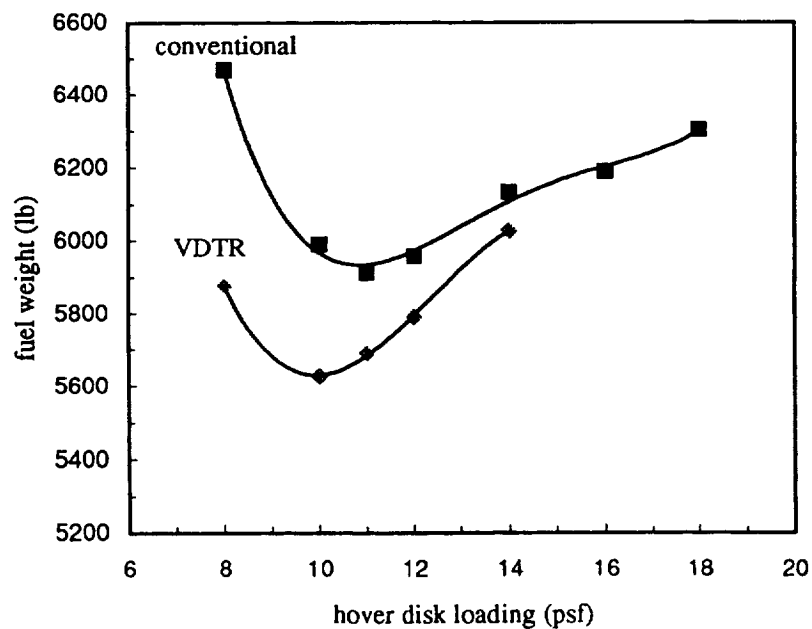


Figure 5.6: VASCOMP Calculated Fuel Weight

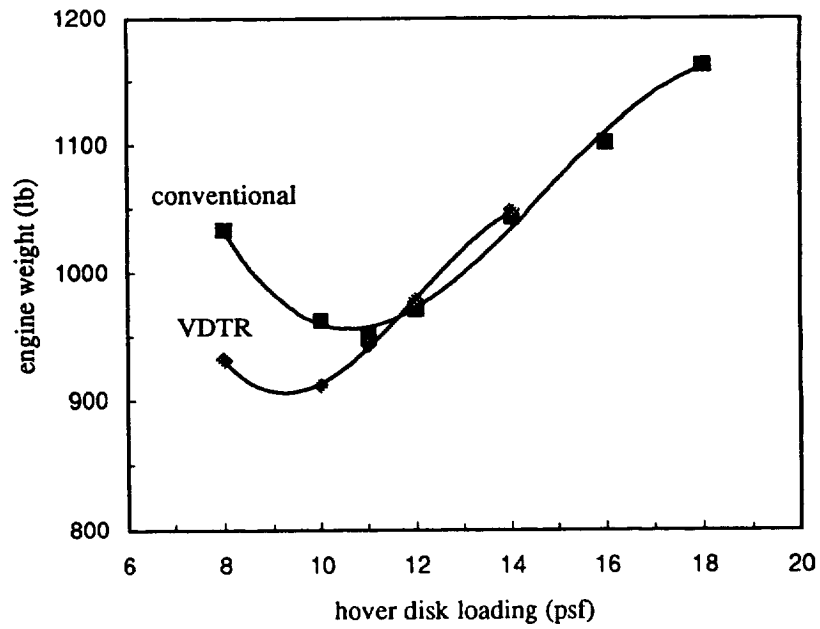


Figure 5.7: VASCOMP Calculated Engine Weight

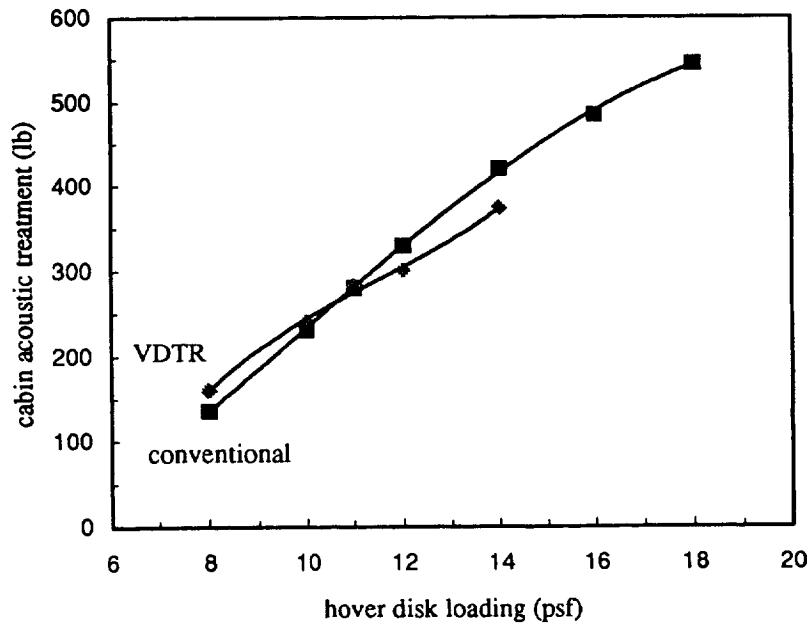


Figure 5.8: VASCOMP Calculated Acoustic Treatment Weight

The fuel savings indicate that the VDTR compares well with a conventional design of the same disk loading. This trend is particularly true when the disk loading is below 11.0 psf. At 10.0 psf the VDTR design has a 6 percent lower fuel weight and 5 percent lower engine weight than the similar conventional design.

For disk loadings from 11-14 psf, the results also show that a conventional design has surprisingly good characteristics. The conventional designs in this range have a beneficial reduction in fuel weight and engine size compared the conventional baseline. Both traits could improve tiltrotor viability. As mentioned before, these results must be used with caution because of likely inaccuracies in the rotor system and wing weight calculations. For instance, if the actual wing or rotor weights were higher, it would not be advantageous to use a high wing aspect ratios to reduce cruise power. The actual engine weight and fuel consumption would then be higher than indicated.

Chapter 6

Conclusions and Recommendations

The VDTR concept offers potential performance and safety benefits for the civil tiltrotor providing system reliability and maintainability can be established. The tradeoffs between weight and performance of the variable-diameter rotor have been quantified in terms of baseline aircraft gross weight, power required, fuel required and landing flare index during autorotation. Other design characteristics have been compared on a qualitative basis including external and internal noise, autorotative steady descent rate, OEI Category A performance and gust response. Definite conclusions about VDTR viability will require further analytical studies, wind tunnel tests, simulations and flight tests as necessary. Questions about the complexity, cost and reliability of a variable-diameter rotor must be answered by the construction and thorough testing of rotor system hardware.

6.1 Conclusions

The results of this study indicate that from the standpoint of safety during power failure, fuel economy, hover power required and wing and engine development costs

the VDTR baseline may be more viable for a larger platform civil mission than the conventional baseline.

The VDTR has a large advantage in OEI Category A performance. Based on beneficial interference effects between the rotors and the hover power calculated by VASCOMP, the VDTR baseline should have a 33 percent lower power requirement at advance ratios in the 0.09 range. Therefore, the VDTR will have an OEI Category A performance without a requirement for high levels of contingency power. This may save on engine development costs and improve engine reliability.

All indications are that a VDTR will provide autorotative performance similar to that of current heavy helicopter designs. The calculated Autorotative Index based on VASCOMP rotor weights for the baseline VDTR was 21 ft³/lb which is comparable to the index of heavy helicopters. In contrast, the conventional rotor design will likely have a very limited autorotative capability. The Autorotative Index for this design was only 9.5 ft³/lb, far below the acceptable range for helicopters. Although the steady autorotative rate of descent was not calculated directly for either baseline, it is evident that the VDTR will descend slower than a conventional design. This conclusion is based on analytical predictions of isolated rotor performance in autorotation discussed previously [29].

Conclusions about the environmental acceptability of either design must await acoustics testing of the rotor systems. Both baseline aircraft are low noise designs, but the VDTR should have advantages in BVI noise. Current analytical methods cannot accurately predict noise from this source.

Conclusions about the overall economic viability of the VDTR are somewhat limited, however, the VDTR baseline was found to be superior in the areas of wing weight, engine size required and fuel economy. The wing of the VDTR design was

sized by bending and shows no need of aeroelastic tailoring. The conventional wing may require more advanced composite designs in order to keep the wing weight acceptable. Also the VDTR was found to require 615 lb less fuel for the same 600 nautical mile mission. The savings in fuel would lead to a small decrease in direct operating cost if all other factors are equal. The VDTR should also improve passenger comfort due to lower gust response as shown in Fig [2.7]. To make an assessment of the overall economic viability, the development and maintenance costs of the variable-diameter mechanism must be known relative to the costs of additional technologies required by conventional designs. The additional costs of conventional designs may include aeroelastic tailoring of wings and development of engines with high contingency power ratings.

If conversion power is similar to hover power as indicated by recent tests of the VDTR in the vertical motion simulator, the VDTR baseline gross weight will be 3.7 percent lower than indicated. This possible reduction in gross weight will amplify the benefits just discussed.

Additional complexity does not necessarily mean the reliability and maintenance costs of the variable-diameter rotor are unacceptable. The current scaled model rotor has redundant load paths so that a single component failure would not cause the rotor to fail. Acceptable reliability may be relatively easy to achieve since the mechanism is only operated during conversion. None of the full-scale risk reduction or model-scale wind tunnel tests discussed in references [14, 16 and 19] have indicated problems in the extension and retraction mechanism.

Low disk loading conventional rotor designs were also investigated as a possible means of improving tiltrotor viability for the civil transport mission. These designs

compared well in terms of gross weight, engine size and power requirement up to a hover disk loading of 11.0 psf.

6.2 Recommended Research

To validate the results of this study and to investigate the viability of the VDTR, further research is necessary in the form of analytical studies, wind tunnel tests, simulation studies and flight tests. 1) Analytical studies would be helpful to improve the accuracy of VASCOMP calculations in areas such as rotor performance, wing and rotor weights and noise. 2) Wind tunnel tests are needed to confirm analytical predictions about the performance of VDTR and about the performance and stability of low disk loading conventional designs. 3) Simulation studies based on mathematical models validated by wind tunnel test data would then be appropriate to determine pilot and passenger opinion of ride quality and emergency landing characteristics. 4) Eventually a flight test demonstrator of the most promising rotor design or designs will be warranted to demonstrate the civil tiltrotor concept and to measure public response to tiltrotor external noise.

1. Several analytical studies should be performed to validate the assumptions of this study and to improve future size and performance calculations. For a more in depth conceptual design analysis, the tiltrotor noise prediction module developed by Wells, Bona and Glinka [40] should be incorporated into VASCOMP. This would involve eliminating redundant calculations and modifying the module to also estimate near field rotor noise. Also, more accurate rotor performance data should be included in VASCOMP for use in calculating cruise and hover efficiency. VASCOMP is already

set up to calculate rotor performance from tables of C_p as a function of μ and C_T . In the absence of wind tunnel test data, sophisticated aerodynamics programs could be used to generate this data for promising rotor designs. The VASCOMP conversion module and the VMS mathematical model should be compared to determine the source of the discrepancy in the conversion power requirement. Blade loads and stability of rotor-wing combinations sized by VASCOMP should be verified using a more sophisticated aeroelastic analysis. The analysis would provide more appropriate reference frequency ratios for use in the VASCOMP wing weight module and indicate possible errors in rotor system weight estimation. This would permit the study of tiltrotor configurations outside the range of experience and determine whether or not the low-disk-loading conventional-tiltrotor size calculations in this study are realistic. A method for estimating steady descent rate in autorotation for conceptual aircraft sized by VASCOMP should also be developed.

2. Wind tunnel tests are critical to validate the results of analytical studies. Some of the most important quantities to measure are listed here. These are the autorotative thrust capability of various proprotor designs, the effects of rotor-wing interactions in autorotation, BVI noise during descent, download of variable-diameter rotor-wing-fuselage combinations and the reliability of the diameter change mechanism.

3. Modern simulation technology should also play a major role in civil tiltrotor development. Simulations provide the opportunity to subject various CTR designs to the scrutiny of pilots and passengers at a low cost. This is critical since tiltrotor flight characteristics will be unique from other aircraft. Passenger tolerance of aircraft vibration and gust response as well as steep approach and departure paths must be

known before proceeding with more expensive flight tests. The limits of pilot technique during partial and total power failures should be established to assess the safety of various designs.

4. A tiltrotor flight demonstrator will likely be necessary to convince relevant parties of the feasibility of the civil tiltrotor. Passenger and community acceptance of tiltrotor ride quality and external noise must be established before operators will commit to purchasing aircraft. Local transportation authorities must also be convinced that investing in the infrastructure for civil tiltrotors involves acceptable risks. One option for a demonstrator is to equip the XV-15 with variable-diameter rotors for direct noise and performance comparisons with conventional proprotor technology. A limitation of the XV-15 demonstrator would be the inability to measure passenger response. Another option is to convert a V-22 into a demonstrator configured to carry passengers. This option has the advantage of providing a near actual-size demonstrator. A sub-option could be to further modify the V-22 with variable-diameter rotors to validate a decrease in the hover power requirement and thereby increase the useful load capability of the aircraft. This would enable demonstration and evaluation of community acceptance for external noise levels as well as passenger acceptance for internal noise and ride quality in a cabin environment representative of an advanced civil tiltrotor.

Bibliography

- [1] Boeing Commercial Airplane Co., et. al, "Civil Tiltrotor Missions and Applications: A Research Study." NASA CR 177451, November, 1987.
- [2] Boeing Commercial Airplane Co., et. al, "Civil Tiltrotor Missions and Applications, Phase II: The Commercial Passenger Market", NASA CR 177576, February 1991.
- [3] "Final Report of the Task Force on High Speed Rotorcraft", Aeronautics Advisory Committee, National Aeronautics and Space Administration, August 1992.
- [4] The Civil Tiltrotor Development Advisory Committee, "Final Report Technical Supplement," Department of Transportation, December, 1995.
- [5] Unger, G., and Alexander, H., "Research Needs for a Commercial Passenger Tiltrotor," *Seventeenth European Rotorcraft Forum*, Paper No. 91-23, Berlin, Germany, September 24-26, 1991.
- [6] *Federal Aviation Regulations*, The Federal Aviation Administration, Department of Transportation.
- [7] *Interim Airworthiness Criteria, Powered-Lift Transport Category Aircraft*, Federal Aviation Administration, Department of Transportation, Southwest Region, Fort Worth, Texas.
- [8] "Technology Needs for High Speed Rotorcraft (3)," NASA Contract Report 177592, October, 1991.
- [9] Schleicher, D., "Advanced Civil Tiltrotor Design Optimization and Issues," *49th Annual Forum of the American Helicopter Society*, St. Louis, MO., 1993.
- [10] Bilger et al., "Interim Flight Test Data Report for XV-15 Tilt Rotor Research Aircraft," Bell Helicopter Textron Report No. 301-989-010, November 15, 1979.
- [11] Fradenburgh, E., and Matuska, D., "Advancing Tiltrotor State-of-the-Art with Variable Diameter Rotors," *American Helicopter Society 48th Annual Forum*, Washington, D.C., June, 1992.
- [12] *Jane's All the World's Aircraft 1995-96*, Jane's Information Group, Alexandria, VA, 1995.

- [13] Fradenburgh, E., "Dynamic Model Wind Tunnel Tests of a Variable-Diameter, Telescoping-Blade Rotor System (TRAC Rotor)," Sikorsky Aircraft Division, United Aircraft Corporation; USAAMRDL Technical Report 73-32, Eustis Directorate, U.S. Army Air Mobility R&D Laboratory, Fort Eustis, VA, July, 1973.
- [14] Frint, H., "Design Selection Tests for TRAC Retraction Mechanism," Sikorsky Aircraft Division, United Technologies Corporation; USAAMRDL Technical Report 76-43, Eustis Directorate, U.S. Army Air Mobility R&D Laboratory, Fort Eustis, VA, January, 1977.
- [15] Martin, S. and Hall, G., "Rotor Will Retract in Flight to Improve V/STOL Cruise Performance," *Space/Aeronautics*, November 1969.
- [16] Fradenburgh, E., "Evaluation of the TRAC Variable Diameter Rotor: Preliminary Design of a Full-Scale Rotor and Parametric Mission Analysis Comparisons," Sikorsky Aircraft Division, United Aircraft Corporation; USAAMRDL Technical Report 75-54, Eustis Directorate, U.S. Army Air Mobility R&D Laboratory, Fort Eustis, VA, February, 1976.
- [17] Cassarino, S., Effect of Root Cutout on Hovering Performance, Sikorsky Aircraft Division of United Aircraft Corporation, Technical Report AFFDL-TR-70-70, Air Force Flight Dynamics Laboratory, Wright Patterson Air Force Base, OH, June 1970.
- [18] Warburton, F. and Curtis, H., "Evaluation of Tiltrotor Aircraft Design Utilizing a Realtime Interactive Simulation," *American Helicopter Society 48th Annual Forum*, Washington, DC., June, 1992.
- [19] Studebaker, K. and Matuska, D., "Variable Diameter Tiltrotor Wind Tunnel Test Results," *American Helicopter Society 49th Annual Forum*, St. Louis, MO, May, 1993.
- [20] Owen, S., "Design and Experimental Verification of a Family of High-Speed Tilt Rotor Airfoils," *American Helicopter Society 51st Annual Forum*, Ft. Worth, TX, May 1995.
- [21] Davis, S., et al., "Aerodynamic Design Optimization of a Variable Diameter Tilt Rotor," *American Helicopter Society 51st Annual Forum*, Fort Worth, TX, May, 1995.
- [22] Johnson, W., *Helicopter Theory*, Princeton University Press, Princeton, 1980.
- [23] McCormick, B., *Aerodynamics of V/STOL Flight*, Academic Press, Inc., San Diego, 1967.
- [24] Felker, F. and Light, J., "Rotor/Wing Aerodynamic Interactions in Hover," *American Helicopter Society 42nd Annual Forum*, Washington, D.C., June 2-4, 1986.

- [25] Felker, F. and Light, J., "Aerodynamic Interactions Between a Rotor and Wing in Hover," *Journal of the American Helicopter Society*, Vol. 33, No. 2, April 1988.
- [26] Pollack, M., Warburton, F. and Curtiss, H., "A Simulation Study of Tiltrotor Vertical Takeoff Procedures Using Conventional and Variable Diameter Rotor Systems," *Seventeenth European Rotorcraft Forum*, Berlin, Germany, September 24-26, 1991.
- [27] Felker, F., "Results from a Test of a 2/3-Scale V-22 Rotor and Wing in the 40-By 80-Foot Wind Tunnel," *American Helicopter Society 47th Annual Forum*, Phoenix, AZ, May 6-8, 1991.
- [28] Dadone, L., Liu, J., Wilkerson, J., and Acree, C., "Proprotor Design Issues for High Speed Tiltrotors," *American Helicopter Society 50th Annual Forum*, Washington, D.C., May 1994.
- [29] Matuska, D., "Issues Pertaining to Tiltrotor Autorotative Capability", Briefing Material Presented to the CTRDAC Environmental/Safety Subcommittee Meeting, Sikorsky Aircraft Corporation, June 6, 1995.
- [30] Fradenburgh, E., "A Simple Autorotative Flare Index," *Journal of the American Helicopter Society*, 29-3, 1984.
- [31] Edwards, B., "XV-15 Tiltrotor Aircraft Noise Characteristics," *American Helicopter Society 46th Annual Forum*, Washington D.C., May 1990.
- [32] Hardin, J. and Lamkin, S., "Concepts for Reduction of Blade-Vortex Interaction Noise," AIAA Paper 86-1855, July 1986.
- [33] Hoad, D., "Helicopter Model Scale Results of Blade-Vortex Interaction Impulsive Noise as Affected by Tip Modification," *American Helicopter Society 36th Annual Forum*, Washington D.C., May 1980.
- [34] Schoen, A., Rosenstein, H., Stanzione, K. and Wisniewski, J., "User's Manual for VASCOMP II, The V/STOL Aircraft Sizing and Performance Computer Program (Revision III)," NASA Contract No. NAS 2-3142, May 1980.
- [35] Phillips, J., "A Robust Numerical Optimizer," AIAA Paper No. 94-4336, 1994.
- [36] Davis, S. and Wisniewski, J., "User's Manual for HESCOMP, The Helicopter Sizing and Performance Computer Program," NASA CR-152018, September, 1973.
- [37] Chappell, D. and Peyran, R., "Methodology for Estimating Wing Weights for Conceptual Tilt-Rotor and Tilt-Wing Aircraft," *51st Annual Conference of Society of Allied Weight Engineers, Inc.*, Hartford, CT, 18-20 May 1992.

- [38] Drees, J., "Prepare for the 21st Century-The 1987 Alexander A. Nikolsky Lecture," *Journal of the American Helicopter Society*, Vol. 32, No. 3, July 1987.
- [39] Talbot, P., Bowles, J., and Lee, H., "Helicopter Rotor and Engine Sizing for Preliminary Performance Estimation," AIAA Paper 86-1756, 1986.
- [40] Wells, V., Bona, J., and Glinka, A., "An Acoustic Methodology for Use in Conceptual Design of Tilt-Rotor Aircraft," *American Helicopter Society 52nd Annual Forum*, Washington, D.C., June 1996.
- [41] Agnihotri, A., Schuessler, W., and Marr, R., "V-22 Aerodynamic Loads Analysis and Development of Loads Alleviation Flight Control System," *American Helicopter Society 45th Annual Forum*, Boston, MA, May 1989.